© 2018. Published by The Company of Biologists Ltd | Development (2018) 145, dev165456. doi:10.1242/dev.165456

RESEARCH ARTICLE

SP8 and SP9 coordinately promote D2-type medium spiny neuron production by activating *Six3* expression

Zhejun Xu[1,*], Qifei Liang[1,*], Xiaolei Song[1,*], Zhuangzhi Zhang[1], Susan Lindtner[2], Zhenmeiyu Li[1], Yan Wen[1], Guoping Liu[1], Teng Guo[1], Dashi Qi[1], Min Wang[1], Chunyang Wang[1], Hao Li[1], Yan You[1], Xin Wang[1], Bin Chen[3], Hua Feng[4], John L. Rubenstein[2] and Zhengang Yang[1,‡]

ABSTRACT

Dopamine receptor DRD1-expressing medium spiny neurons (D1 MSNs) and dopamine receptor DRD2-expressing medium spiny neurons (D2 MSNs) are the principal projection neurons in the striatum, which is divided into dorsal striatum (caudate nucleus and putamen) and ventral striatum (nucleus accumbens and olfactory tubercle). Progenitors of these neurons arise in the lateral ganglionic eminence (LGE). Using conditional deletion, we show that mice lacking the transcription factor genes *Sp8* and *Sp9* lose virtually all D2 MSNs as a result of reduced neurogenesis in the LGE, whereas D1 MSNs are largely unaffected. SP8 and SP9 together drive expression of the transcription factor *Six3* in a spatially restricted domain of the LGE subventricular zone. Conditional deletion of *Six3* also prevents the formation of most D2 MSNs, phenocopying the *Sp8*/*9* mutants. Finally, ChIP-Seq reveals that SP9 directly binds to the promoter and a putative enhancer of *Six3*. Thus, this study defines components of a transcription pathway in a regionally restricted LGE progenitor domain that selectively drives the generation of D2 MSNs.

KEY WORDS: *Sp8*, *Sp9*, *Six3*, LGE, DRD2, Striatum, Medium spiny neuron, Mouse

INTRODUCTION

The striatal subdivisions – the caudate nucleus, putamen (caudate-putamen), nucleus accumbens and olfactory tubercle – are key components of distributed circuits integral to cognitive, motor and reward processes. Their dysfunction contributes to brain disorders, such as Huntington's and Parkinson's disease, and addiction (Kreitzer and Malenka, 2008; Maia and Frank, 2011). There are two major cell types of medium spiny neurons (MSNs), the principal projection neurons of the striatum: dopamine receptor DRD1-expressing MSNs (D1 MSNs) and dopamine receptor DRD2-expressing MSNs (D2 MSNs). Although these GABAergic neurons share many properties, they have some distinct molecular properties and differentially contribute to distinct circuits (e.g. direct and indirect pathway) (Lobo et al., 2006; Heiman et al., 2008; Gerfen and Surmeier, 2011; Ena et al., 2013; Gokce et al., 2016; Merchan-Sala et al., 2017).

Transcriptional control of MSN development occurs in the lateral ganglionic eminence (LGE), and involves a cascade of transcription factors (TFs), including GSX1/2, DLX1/2/5/6, ASCL1, EBF1 and ISL1 (Rubenstein and Campbell, 2013). Previously, we reported that the zinc finger TF gene *Sp9* is expressed in subventricular zone (SVZ) progenitors of both D1 and D2 MSNs, and its expression persists in the postmitotic D2 MSNs but not in D1 MSNs (Zhang et al., 2016). We demonstrated that *Sp9* is required for the generation, differentiation and survival of D2 MSNs, as ∼95% of them are lost in the caudate-putamen of *Sp9* null mutants (Zhang et al., 2016). We also showed that SP9 promotes the expression of *Drd2*, *Adora2a*, *P2ry1*, *Gpr6* and *Grik3* genes, which are specific molecular markers for D2 MSNs (Zhang et al., 2016). Currently, SP9 is the only TF that has been shown to control the expression of D2 MSN terminal differentiation genes.

The LGE progenitor zone is proposed to be organized into four domains along the dorsoventral axis (pLGE1, 2, 3 and 4) (Flames et al., 2007). Whereas *Sp9* is broadly expressed in all pLGE domains in the SVZ, its paralog, *Sp8*, is most prominently expressed dorsally (dorsal LGE, dLGE), in the SVZ of pLGE1 and pLGE2. *Sp8* and *Sp9* are co-expressed prenatally and postnatally in the SVZ, rostral migratory stream (RMS) and olfactory bulb (OB) interneurons (Long et al., 2007; Li et al., 2017). Together, *Sp8* and *Sp9* regulate OB interneuron differentiation, tangential and radial migration, and survival by promoting *Prokr2* and *Tshz1* expression (Li et al., 2017). In the absence of *Sp8* and *Sp9*, immature OB interneurons fail to express *Prokr2* and *Tshz1*, genes that are required for OB interneuron development and are involved in human Kallmann syndrome (Li et al., 2017).

The ventral LGE (vLGE, i.e. pLGE3 and pLGE4) domains generate MSNs (Toresson and Campbell, 2001; Stenman et al., 2003; Silberberg et al., 2016). *Sp9* is broadly expressed in the SVZ of these domains, whereas *Sp8* appears to be weakly expressed in the SVZ of pLGE3 (Waclaw et al., 2006; Ma et al., 2012). The function and targets of SP8 in the vLGE are unknown.

Here, we analyzed the generation of D1 and D2 MSNs in the caudate-putamen, nucleus accumbens and olfactory tubercle in *Sp8*, *Sp9* and *Sp8/Sp9* mutant mice [*Dlx5/6-CIE; Sp8*$^{F/F}$ (hereafter referred to as *Sp8-CKO*), *Sp9*$^{lacZ/lacZ}$ null mutant (*Sp9-KO*) and *Dlx5/6-CIE; Sp8*$^{F/F}$*; Sp9*$^{F/F}$ double conditional knockout (*Sp8/9-DCKO*)]. *Sp8/9-DCKO* mice, compared with *Sp8-CKO* and *Sp9-KO*, have a more severe reduction of D2 MSNs. This is mainly due to severely reduced LGE neurogenesis. Crucially, *Sp8* and *Sp9* are required for expression of the TF *Six3* in the SVZ of

[1]State Key Laboratory of Medical Neurobiology, Institutes of Brain Science, Department of Neurology, Zhongshan Hospital, Fudan University, Shanghai 200032, China. [2]Department of Psychiatry, Nina Ireland Laboratory of Developmental Neurobiology, UCSF Weill Institute for Neurosciences, University of California, San Francisco, CA 94158, USA. [3]Department of Molecular, Cell and Developmental Biology, University of California, Santa Cruz, CA 95064, USA. [4]CAS Key Laboratory of Computational Biology, CAS-MPG Partner Institute for Computational Biology, Shanghai Institutes for Biological Sciences, Chinese Academy of Sciences, Shanghai 200031, China.
*These authors contributed equally to this work

‡Author for correspondence (yangz@fudan.edu.cn)

Z.Y., 0000-0003-2447-6540

Received 10 March 2018; Accepted 18 June 2018

Development (2018) 145, dev165456. doi:10.1242/dev.165456

pLGE3. *Six3* belongs to the Six/sine oculis family of homeobox TFs; it promotes cell proliferation and differentiation (Oliver et al., 1995; Kobayashi et al., 1998; Loosli et al., 1999; Del Bene et al., 2004; Del Bene and Wittbrodt, 2005; Appolloni et al., 2008). We show that *Six3-CKO* mice (*Dlx5/6-CIE; Six3*$^{F/F}$) lose the majority of D2 MSNs, phenocopying *Sp8/9-DCKO* mice. Finally, chromatin co-immunoprecipitation combined with followed by high-throughput DNA sequencing (ChIP-Seq) reveals that SP9 directly binds to the promoter and a putative enhancer of *Six3*, providing evidence that SP9 regulates D2 MSN development by direct regulation of *Six3* expression. Thus, we provide evidence for components of a transcription pathway, in a regionally restricted LGE domain, that selectively drives the generation of D2 MSNs.

RESULTS

SP8 expression is upregulated in the *Sp9-KO* LGE SVZ and striatum

SP8 protein is strongly expressed in the dLGE SVZ and weakly expressed in the vLGE SVZ (Fig. 1A-H) (Waclaw et al., 2006; Ma et al., 2012). Most SP8^{+} cells (>91%) in the LGE SVZ expressed SP9 at embryonic day (E) 14.5 and E16.5 (Fig. 1D,H), whereas only a few SP8^{+} cells expressed ASCL1, a marker for neural progenitors (Fig. S1A-D). SP8 expression in MSNs is at background levels (Fig. 2A,B). In contrast, SP9 is strongly expressed in the SVZ of both the dLGE and the vLGE, and its expression is maintained in the D2 MSNs but not in D1 MSNs (Fig. 1A-H, Figs S1E-H, S2A) (Zhang et al., 2016).

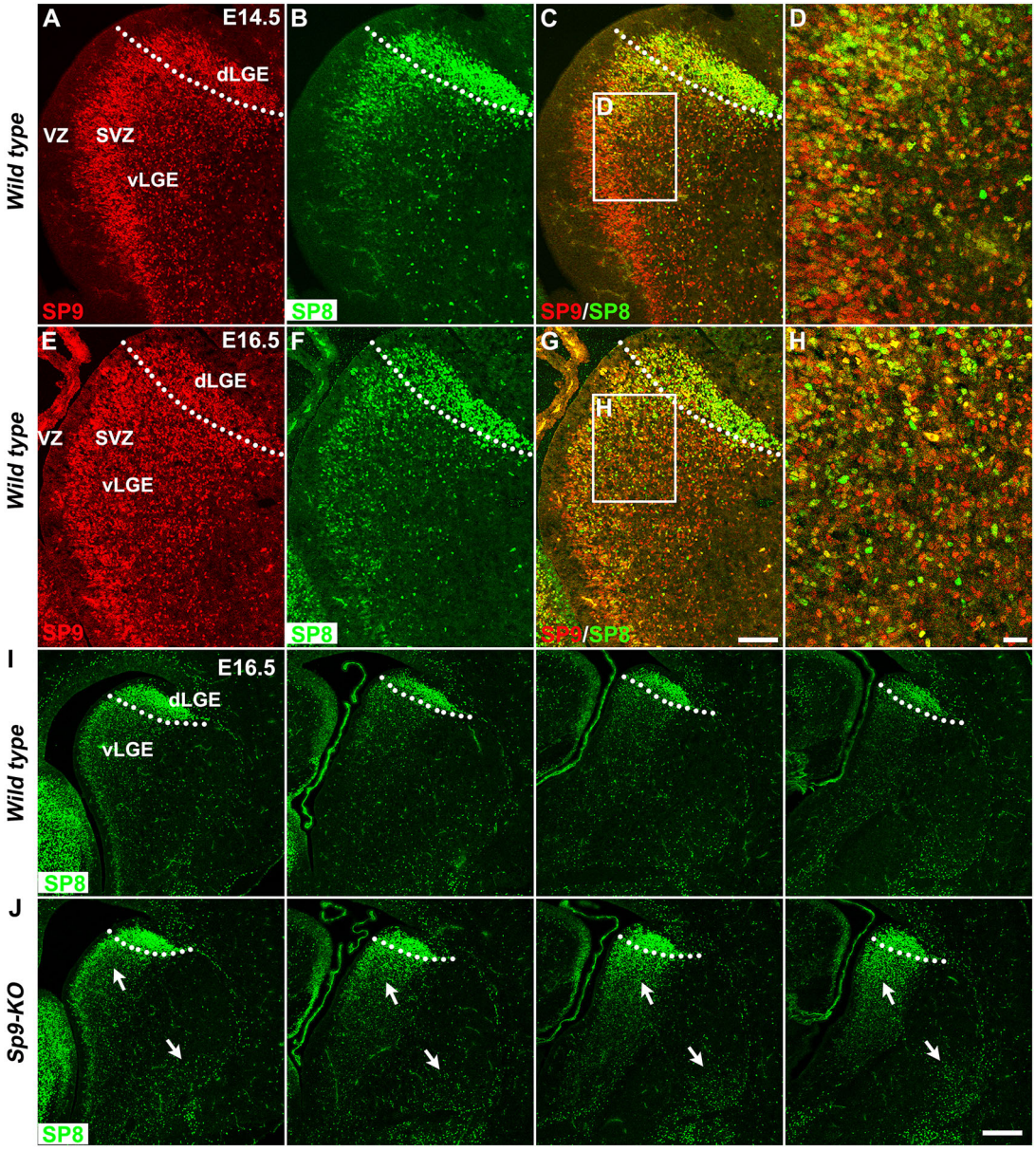

Fig. 1. Most SP8^{+} cells in the LGE SVZ express SP9. (A-H) Co-expression of SP8 and SP9 in the LGE SVZ at E14.5 and E16.5. Note that SP8 is strongly expressed in the dLGE SVZ, and weakly expressed in the vLGE SVZ, but most SP8^{+} cells express SP9. (I,J) SP8 expression in the E16.5 LGE SVZ (rostral to the left) of wild-type and *Sp9-KO* mice. Arrows indicate upregulation of SP8 in the LGE. Dotted line indicates the border of the dorsal and ventral LGE. Scale bars: 100 µm in G for A-C,E-G; 20 µm in H for D,H; 200 µm in J for I,J.

Development (2018) 145, dev165456. doi:10.1242/dev.165456

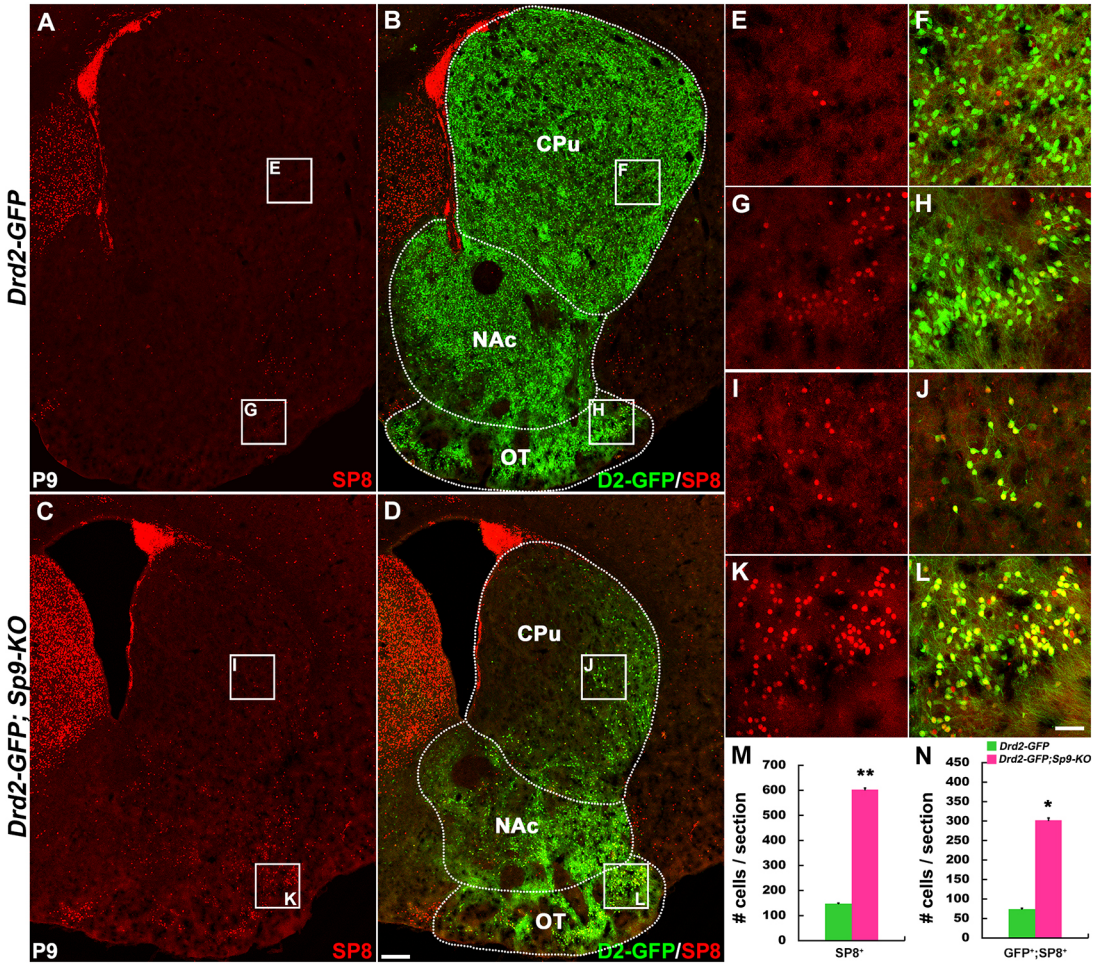

Fig. 2. The *Sp9-KO* striatum has more SP8$^+$/DRD2-GFP$^+$ MSNs. (A-D) SP8/GFP double immunostained coronal striatal sections of *Drd2-GFP* control and *Drd2-GFP; Sp9$^{lacZ/lacZ}$* (*Sp9-KO*) mutant mice at P9. (E-L) Higher magnification images of the boxed areas in A-D. (M,N) Quantification data showing that *Sp9-KO* mice had more SP8$^+$ and SP8$^+$/DRD2-GFP$^+$ cells in the striatum per section than controls (Student's *t*-test, **P*<0.05, ***P*<0.01, *n*=3, mean+s.e.m.). CPu, caudate-putamen; NAc, nucleus accumbens; OT, olfactory tubercle. Scale bars: 200 µm in D for A-D; 50 µm in L for E-L.

In the *Sp9-KO* embryos, SP8 expression is upregulated in the SVZ of both the dLGE and vLGE at E14.5 (Fig. S2B,C) and E16.5 (Fig. 1I,J, arrows). In the postnatal striatum of *Drd2-GFP* transgenic mice, only a small number of DRD2-GFP$^+$ cells expressed SP8 (Fig. 2A,B,E-H). Although D2 MSNs were severely reduced in the striatum of *Sp9-KO; Drd2-GFP* mice, the number of SP8$^+$ and DRD2-GFP$^+$/SP8$^+$ neurons showed a ∼4-fold increase (Fig. 2C,D, I-N). The DRD2-GFP$^+$ cells in the caudate-putamen of *Sp9-KO* mice that do not express SP8 are choline acetyltransferase (ChAT)$^+$ interneurons (Zhang et al., 2016). The fact that the majority of the D2 MSNs that remained in the *Sp9-KO* striatum upregulated SP8 expression suggests that SP8 could be compensating for SP9 function. Thus, given their sequence homology, and LGE expression, *Sp8* and *Sp9* may share functions in regulating MSN development. To test this hypothesis, we compared MSN development in control (*Dlx5/6-CIE*), *Sp8-CKO*, *Sp9-KO* and *Sp8/9-DCKO* mice.

Nearly all D2 MSNs are lost in *Sp8/9-DCKO* mice whereas D1 MSNs are less affected in *Sp8-CKO*, *Sp9-KO* and *Sp8/9-DCKO* mice

We first examined the D2 MSNs in the control and mutant striatum at postnatal day (P) 11, as most *Sp8/9-DCKO* mice die at P12. *Drd2*, *Adora2a*, *Penk* and *Gpr6* are expressed by D2 MSNs (Fig. 3A-J, Fig. S3A-L). *In situ* RNA hybridization of *Drd2* and *Adora2a* revealed that only ∼5% of D2 MSNs were lost in the *Sp8-CKO* striatum (Fig. 3A-J). In the *Sp9-KO* striatum, in contrast, ∼85% D2 MSNs were lost; the remaining D2 MSNs were mainly located in the ventral and lateral striatum (Fig. 3C,H) (Zhang et al., 2016). In *Sp8/9-DCKO* mice, we did not observe *Adora2a*$^+$ or *Gpr6*$^+$ cells in the striatum, suggesting a lack of D2 MSNs (Fig. 3I, Fig. S3L). Some neurons in the *Sp8/9-DCKO* striatum retained *Drd2* expression but they were ChAT$^+$ interneurons (Fig. S4A-H) (Durieux et al., 2009; Zhang et al., 2016). At P0, *Sp8/9-DCKO* mice was also lacked molecular markers of D2 MSNs (Fig. S5A-P).

We next examined the D1 MSNs in the mutant striatum. *In situ* hybridization of *Drd1* and *Tac1* (tachykinin precursor 1) revealed that, relative to controls, striatal D1 MSNs were largely unaffected in *Sp8-CKO*, *Sp9-KO* and *Sp8/9-DCKO* mice at P11 (Fig. 3K-T). Similar results were also observed at P0 (Fig. S5Q-X). Taken together, our results support the hypothesis that *Sp8* and *Sp9* have redundant and essential functions in generating D2 MSNs, whereas they only have minor roles in the development of D1 MSNs.

RNA-Seq confirms loss of D2 MSNs and reveals reduced neurogenesis in the LGE of *Sp8/9-DCKO* mice

To define the transcriptional changes in the LGE of *Sp8/9-DCKO* in order to elucidate the mechanisms underlying the preferential loss of

Development (2018) 145, dev165456. doi:10.1242/dev.165456

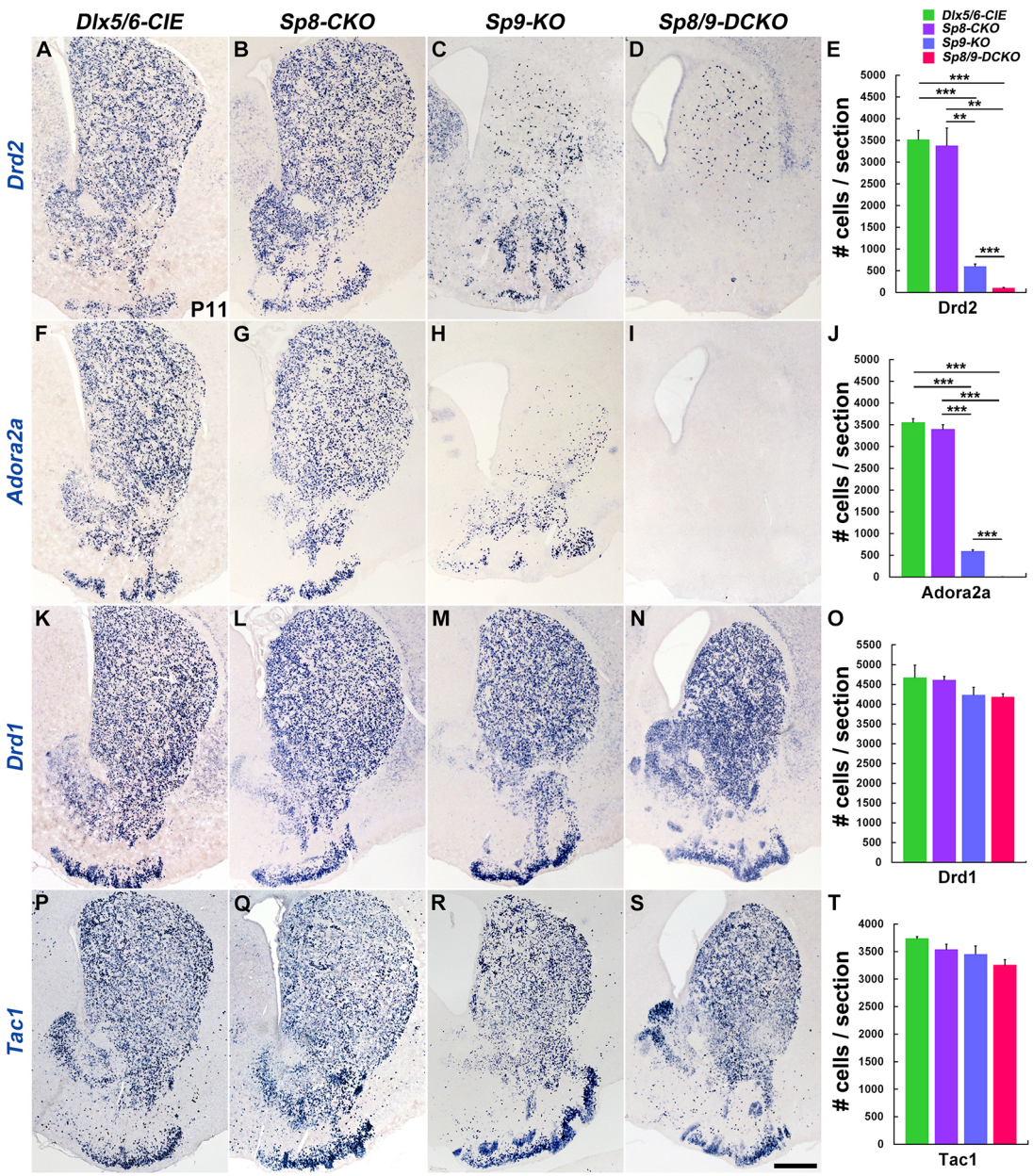

Fig. 3. *Sp8/9-DCKO* mice lose nearly all D2 MSNs. (A-J) *In situ* RNA hybridization of *Drd2* and *Adora2a* showed that nearly all D2 MSNs were lost in the striatum at P11. Those remaining *Drd2*$^{+}$ cells in the *Sp8/9-DCKO* striatum (D) are ChAT^{+} interneurons. (K-T) *Drd1* and *Tac1* mRNA in the striatum of control and mutant mice at P11. The generation of D1 MSNs was largely unaffected in mutant mice relative to controls. (E,J,O,T) Histograms showing quantification of the data (one-way ANOVA followed by Tukey–Kramer post-hoc test, ***P*<0.01, ****P*<0.001, *n*=3, mean+s.e.m.). Scale bar: 500 µm in S for A-D,F-I,K-N,P-S.

D2 MSNs, we compared control and *Sp8/9-DCKO* transcriptomes by RNA sequencing (RNA-Seq). Gene expression profiles from the E16.5 LGE [including the VZ (ventricular zone), SVZ and MZ (mantle zone)] of *Sp8/9-DCKO* mice and littermate controls (*Sp8/9* floxed mice without *Dlx5/6-CIE* allele) (*n*=3 biological replicas) were analyzed. Gene expression levels are reported in fragments per kilobase of exon per million fragments mapped (FPKM) (Trapnell et al., 2012; Li et al., 2017) (Table S1). For example, the expression levels (FPKM) of *Sp8* and *Sp9* genes in the control mouse LGE at E16.5 were 7.7 and 137.8, respectively, whereas their expression levels in the *Sp8/9-DCKO* LGE were reduced to 0.7 and 1.4 (Table S1). Thus, as expected, the mutation greatly reduced *Sp8* and *Sp9* LGE expression. About 80 genes were downregulated and 120 genes were upregulated (*P*<0.05, Student's *t*-test).

Next, we analyzed the expression of D2 MSN-enriched genes, and found that *Adora2a*, *Drd2*, *Gpr6*, *Penk* and *Ptprm* RNA was near background levels in the mutants (Table S1), supporting the evidence that D2 MSNs were not generated in the *Sp8/9-DCKO* mice. In contrast, the expression of D1 MSN-enriched genes, such as *Drd1*, *Pdyn*, *Isl1*, *Ebf1* and *Sox8*, were largely unaffected (Table S1).

RNA levels of pan-neuronal genes (*Gad1*, *Dcx*, *Bcl11a*, *Bcl11b*, *Foxp1*, *Meis2*, *Rxrg* and *Tubb3*) were also reduced (Table S1), further supporting the suggestion that striatal MSN neurogenesis is comprised in *Sp8/9-DCKO* mice. In contrast, expression levels of genes that are highly enriched in LGE neural stem/progenitor cells, such as *Gsx1*, *Gsx2*, *Ascl1* (also known as *Mash1*), *Dbi*, *Dlx2*, *Fabp7* (also known as *Blbp*), *Lhx2* and *Vim*, were increased

Development (2018) 145, dev165456. doi:10.1242/dev.165456

(Table S1). The increased expression of progenitor genes and reduced expression of pan-neuronal and D2 MSN genes suggest that lack of *Sp8/9* impedes the ability of neural progenitors to generate D2 MSNs.

Sp8/9 promote neuronal differentiation in the LGE

In *Sp8-CKO* embryos, *in situ* RNA hybridization showed that in the E14.5 and E16.5 LGE (VZ-SVZ) *Gsx2*, *Dlx1*, *Dlx2* and *Ascl1* expression were subtly increased (Fig. 4A-D, Fig. S6A-D). ASCL1 has roles in both cell cycle promotion and cell cycle termination through direct activation of positive and negative cell cycle regulators (Castro et al., 2011). Consistent with this, we observed upregulation of *Ascl1* and its target genes (*E2f1*, *Cdca7*, *Cdk1* and *Hes5*) that promote cell cycle and maintenance of the progenitor state, and its target genes (*Gadd45g* and *Btg2*) that inhibit cell cycle, using *in situ* hybridization on E14.5 *Sp8-CKO* embryos (Fig. S6E-J) (Castro et al., 2011). Thus, upregulation of *Ascl1* in the *Sp8-CKO* mice may contribute to the blockage of neuronal differentiation in the LGE SVZ. Importantly, misregulation of this *Ascl1* pathway in neural progenitors was not apparent in *Sp9-KO* mice, but was more even severe in *Sp8/9-DCKO* than the *Sp8-CKO* (Fig. 4A-D, Fig. S6A-J, Table S1). Indeed, quantification of $GSX2^+$ and $ASCL1^+$ cells in the E16.5 LGE VZ and SVZ further demonstrated that there were more neural progenitors in *Sp8-CKO* and *Sp8/9-DCKO* than control and *Sp9-KO* mice (Fig. 4E-P). Together, these results provide evidence that *Sp8* and *Sp9* have different and redundant roles in the generation of D2 MSNs.

Neurogenesis is reduced in *Sp8/9-DCKO* caudate-putamen

We next examined neurogenesis in the caudate-putamen of wild-type control, *Sp8-CKO*, *Sp9-KO* and *Sp8/9-DCKO* mice. The SVZ of the mouse LGE is larger than the SVZ of the cortex (Smart, 1976; Sheth and Bhide, 1997). At early developmental stages, the LGE SVZ has a high density of cycling progenitors, whereas the late SVZ contains relatively more differentiated cells, such as postmitotic $FOXP1^+$ and $EBF1^+$ immature neurons at E16.5 (Fig. 5A,F). *Sp8/9-DCKO* lose most of these $FOXP1^+$ and $EBF1^+$ cells; the single mutants have more subtle reductions (Fig. 5A-J). Expression of DCX and TUBB3 (general markers of immature neurons) was also reduced in the SVZ of *Sp8/9-DCKO* (Fig. 5K-N), supporting the suggestion of a reduction of neurogenesis in the LGE at E16.5.

We determined whether cell cycle exit was affected by *Sp8* and *Sp9* mutations by examining the state of differentiation of cells following a pulse-chase of 5-bromo-2′-deoxyuridine (BrdU) (Fig. 5O-T). In control and *Sp8-CKO* mice at E16.5 (24 h after BrdU injection), most $BrdU^+$ cells were still in the VZ/SVZ, and very few $BrdU^+$ cells were found in the striatum (Fig. 5P,Q). By contrast, in *Sp9-CKO* and *Sp8/9-DCKO* mice, we observed an increase in the number of $BrdU^+$ cells in the striatum (Fig. 5P-T), suggesting a premature differentiation of SVZ progenitors at this age. In contrast, *Sp8-CKO* and *Sp8/9-DCKO* mice had increased numbers of $BrdU^+$ cells in the LGE VZ/SVZ (Fig. 5O). This is consistent with the above observations that more progenitors accumulated in the VZ/SVZ of these mice (Fig. 4, Fig. S6).

To examine further the reduction in striatal neurogenesis, we performed a BrdU birthdating analysis. BrdU was given at E13.5, a

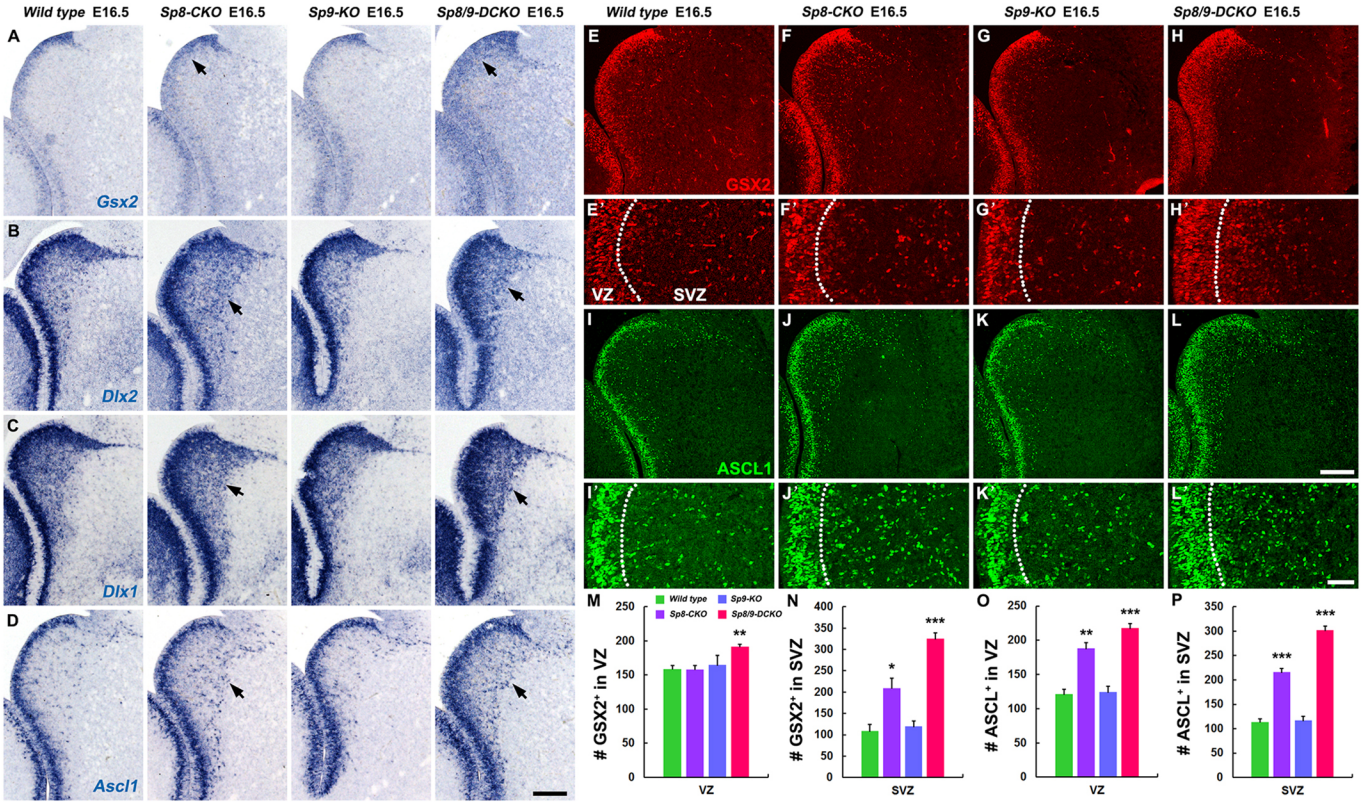

Fig. 4. Accumulation of neural progenitors in the LGE of *Sp8/9-DCKO* mice at E16.5. (A-D) *In situ* RNA hybridization showed that there were more neural stem/progenitor cells ($Gsx2^+$, $Dlx1^+$, $Dlx2^+$ and $Ascl1^+$ cells, arrows) in the LGE VZ/SVZ of *Sp8-CKO* and *Sp8/9-DCKO* mice compared with control and *Sp9-KO* mice. (E-L′) GSX2 and ASCL1 immunostained LGE sections in control and mutant mice. Dotted lines mark the border of the VZ and SVZ of the LGE. (M-P) Quantification data showing that there are more $GSX2^+$ and $ASCL1^+$ neural progenitors in the LGE VZ and SVZ of *Sp8-CKO* and *Sp8/9-DCKO* mice. (one-way ANOVA followed by Tukey–Kramer post-hoc test, $^{**}P<0.01$, $^{***}P<0.001$, $n=3$, mean+s.e.m.). Scale bars: 200 µm in D for A-D; 200 µm in L for E-L; 50 µm in L′ for E′-L′.

Development (2018) 145, dev165456. doi:10.1242/dev.165456

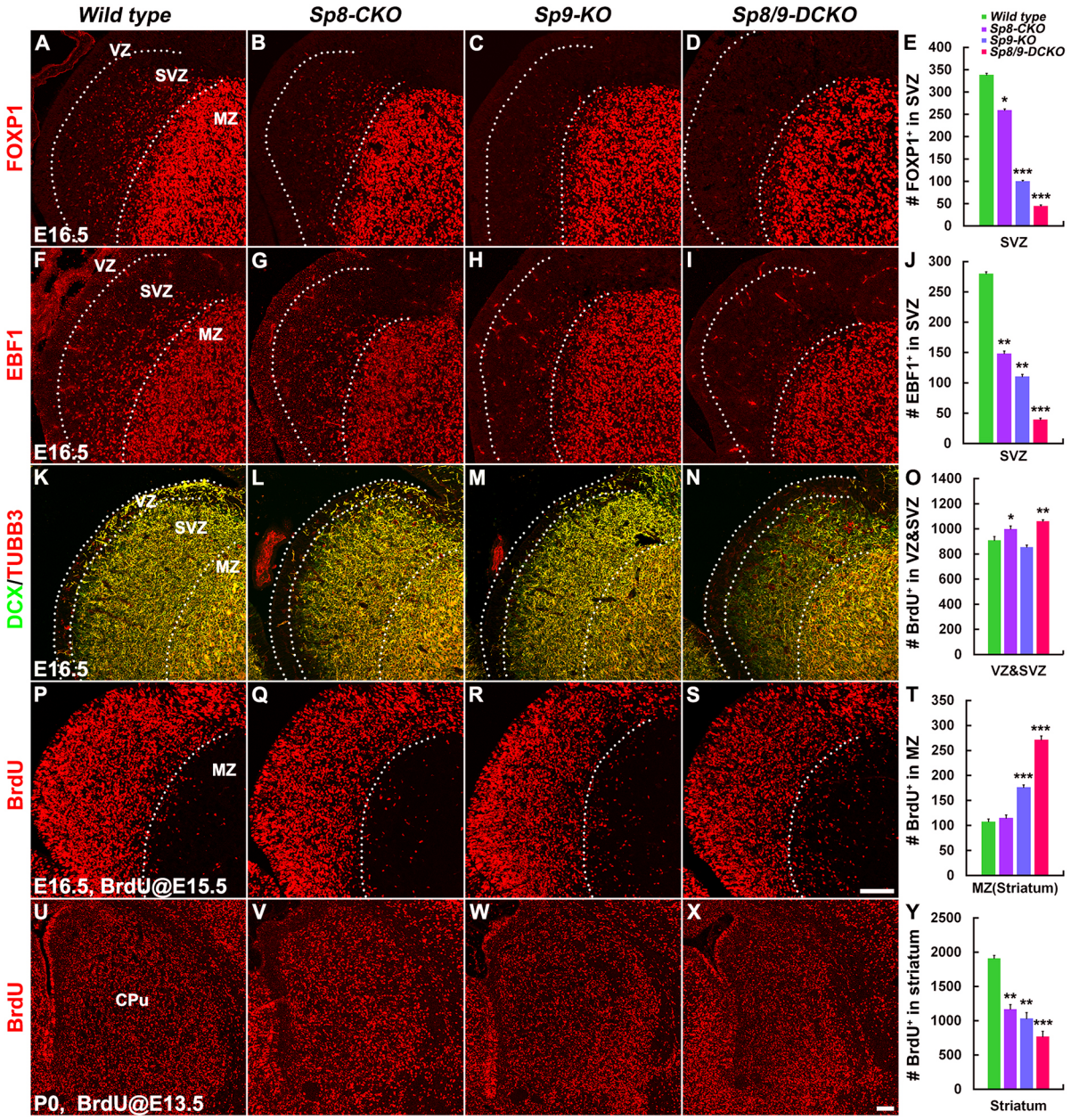

Fig. 5. MSN production is reduced in *Sp8/9-DCKO* mice. (A-J) The *Sp8-CKO*, *Sp9-KO* and *Sp8/9-DCKO* LGE SVZ had fewer FOXP1$^+$ and EBF1$^+$ cells relative to wild-type controls at E16.5. (K-N) DCX and TUBB3 expression was greatly reduced in *Sp8/9-DCKO* LGE SVZ. (O-T) BrdU was injected intraperitoneally at E15.5, and mice were sacrificed at E16.5 (24 h after BrdU injection). *Sp8-CKO* and *Sp8/9-DCKO* embryos had more BrdU$^+$ cells in the LGE VZ/SVZ relative to controls, whereas *Sp9-KO* and *Sp8/9-DCKO* embryos had more BrdU$^+$ cells in the LGE MZ (striatum). (U-Y) BrdU was injected intraperitoneally at E13.5, and then mice were sacrificed at P0. Immunostaining of BrdU showed that mutant mice had reduced BrdU$^+$ cells in the striatum relative to controls. Dotted lines mark the border of the VZ, SVZ and MZ of the LGE. CPu, caudate-putamen. One-way ANOVA followed by Tukey–Kramer post-hoc test, **P*<0.05, ***P*<0.01, ****P*<0.001, *n*=3, mean+s.e.m.). Scale bars: 100 µm in S for A-D,F-I,P-S; in X for U-X.

time point in the middle of the striatal neurogenic period. We then counted the number of BrdU$^+$ cells in the caudate-putamen in P0 tissue sections. *Sp8-CKO*, *Sp9-KO* and *Sp8/9-DCKO* mutants each had reduced BrdU$^+$ cells with *Sp8/9-DCKO* showing the greatest reduction (Fig. 5U-Y). Thus, *Sp8* and *Sp9* both promote MSN production.

Apoptotic cell death occurs in the *Sp8/9-DCKO* caudate-putamen

We recently observed that loss of *Sp9* function induced Bax-dependent apoptosis, as cleaved caspase 3 cells were not observed in the postnatal caudate-putamen of *Sp9-KO; Bax*$^{-/-}$ double mutant mice (Fig. S7Q) (Zhang et al., 2016). We next examined apoptotic cell death in the *Sp8-CKO*, *Sp9-KO* and *Sp8/9-DCKO* caudate-putamen. Compared with control (*Dlx5/6-CIE*) and *Sp8-CKO* mice, there were more caspase 3$^+$ cells in the caudate-putamen of *Sp9-KO* (~3- to 6-fold increase) and *Sp8/9-DCKO* (~3 fold increase) mice at P2 and P3 (Fig. S7A-T). Notably, the number of caspase 3$^+$ cells in the *Sp9-KO* caudate-putamen was larger than that in *Sp8-CKO* and *Sp8/9-DCKOs* at P2 and P3 (Fig. S7R-T). This could be because *Sp9-KO* mice generated more mutant striatal cells relative to *Sp8/9-DCKO* mice (based on our BrdU birthdating analysis, Fig. 5U-Y)

Development (2018) 145, dev165456. doi:10.1242/dev.165456

and a large number of these mutant cells die without *Sp9* function (Zhang et al., 2016). Therefore, we conclude that reduction of striatal MSNs in *Sp8/9*-DCKO mice results from a combination of reduced neurogenesis and apoptosis.

Six3 expression is downregulated in *Sp9-KO* and lost in the *Sp8/9-DCKO* LGE

Accumulation of neural progenitors and upregulation of cell cycle-regulated genes were observed in the LGE of the *Sp8-CKO* and *Sp8/9-DCKO*, but these were not apparent in *Sp9-KO* mutants (Fig. 4, Fig. S6). However, *Sp9-KO* mice generated many fewer MSNs (particularly D2 MSNs) than did *Sp8-CKO* mice (Figs 3A-J, 5U-Y, Fig. S3A-L). This implies that there are additional mechanisms that regulate the generation of D2 MSNs in *Sp9-KO* mice, one of which was suggested by the LGE RNA-Seq analysis. We identified that expression of the TF *Six3* was decreased ∼5-fold in E16.5 *Sp8/9-DCKO* mice compared with control mice (control versus *Sp8/9-DCKO*: FPKM, 64.2 versus 12.7; P=0.000000000857, FDR=0.00000113) (Table S1). *Six3* promotes proliferation and differentiation through both transcription-dependent and -independent mechanisms (Oliver et al., 1995; Kobayashi et al., 1998; Loosli et al., 1999; Del Bene et al., 2004; Del Bene and Wittbrodt, 2005; Appolloni et al., 2008). Furthermore, single-cell RNA-Seq has identified that *Six3* is preferentially expressed in D2 MSNs (Gokce et al., 2016). Therefore, we hypothesized that *Six3* could be a key LGE target of SP8 and SP9 in driving D2 MSN development.

Next, we analyzed *Six3* expression in the LGE of wild-type mice. In the E12.5-E14.5 LGE, *Six3* is weakly expressed in the VZ and strongly expressed in the SVZ (preferentially in pLGE3, the dorsal part of the vLGE), but not in the dLGE (pLGE1 and 2) (Fig. 6A-C, Fig. S8A-D). Scattered *Six3*$^+$ cells were also observed in the immature striatum (Fig. 6A-C, Fig. S8A-E) (Oliver et al., 1995). *Six3* expression was also observed in the VZ of the medial ganglionic eminence (MGE) and preoptic area (POA) (Fig. 6A-C) (Xu et al., 2010; Sandberg et al., 2016).

At E16.5, SIX3 continued to be expressed in the vLGE SVZ, but not in the dLGE (Fig. 6D, Fig. S8F-I). BrdU 30 min pulse-labeling demonstrated that about 9% of SIX3$^+$ cells in the LGE SVZ were in S phase (Fig. 6D-F,K). We found that, in the LGE SVZ, ∼90% SIX3$^+$ cells co-expressed SP9 and ∼80% DRD2-GFP$^+$ cells co-expressed SIX3 (Fig. 6G-M). Furthermore, SP9 expression in the LGE SVZ began before SIX3 (based on the position of the SP9 single-positive cells closer to the VZ; Fig. 6J) and SIX3 expression began before DRD2-GFP (Fig. 6G-I). As SIX3$^+$ cells migrated from the SVZ into the MZ, most of them expressed lower SIX3 levels (Fig. 6A-D,H). SIX3/SP8 double immunostaining revealed that a subset of SP8$^+$ cells in the E13.5 and E16.5 LGE SVZ and MZ also expressed SIX3 (Fig. S8A-J). In contrast, SIX3$^+$ cells in the LGE did not express D1 MSN markers ISL1 or EBF1 (Fig. S9A-F).

Most *Sp8*, *Sp9* and *Sp8/9* mutant cells appear to be present in the mutant LGE SVZ based on *Sp9-lacZ* expression (in *Sp9-KO*), and *Dlx5/6-GFP* expression (in *Sp8-CKO* and *Sp8/9-DCKO*) at E16.5 (Fig. 7A-D) (Zhang et al., 2016). However, *Six3* expression was reduced in the LGE SVZ of *Sp9-KO* mice and was almost undetectable in of *Sp8/9-DCKO* mice, whereas its expression appeared normal in *Sp8-CKO* mice (Fig. 7E-L; Fig. S10A-D). *Six3* expression in the LGE SVZ at E16.5 was also almost undetectable when we used a *Nestin-Cre* transgenic allele to knock out *Sp8* and *Sp9* (Fig. 7M-P). Together, these data show that *Sp9*, together with *Sp8*, promotes *Six3* expression in the SVZ.

Six3-CKO striatum lacks most D2 MSNs

To examine *Six3* function in MSN development, we used *Dlx5/6-CIE* to delete exon 1, which encodes the Six domain and homeodomain of the *Six3* gene (Liu et al., 2006). We analyzed D1 and D2 MSNs in the mutant striatum at P11. More than 90% of *Drd2*$^+$, *Adora2a*$^+$, *Penk*$^+$ and *Gpr6*$^+$ D2 MSNs were lost in the *Six3-CKO* striatum (Fig. 8A-L), whereas the majority of *Drd1*$^+$ and *Tac1*$^+$ D1 MSNs remained (Fig. 8M-R). Thus, the preferential reduction of D2 MSNs in the *Six3-CKO* closely phenocopied the *Sp8/9-DCKO*.

SP9 directly binds to the promoter and a putative enhancer of *Six3* at E13.5 and E16.5

To test the hypothesis that SP9 directly promotes *Six3* expression in the LGE SVZ, we performed ChIP-Seq using E13.5 and E16.5 wild-type ganglionic eminences (LGE+MGE) (McKenna et al., 2011; Sandberg et al., 2016) and an SP9 rabbit polyclonal antibody (Zhang et al., 2016). The presence of an SP9 ChIP-seq peak, combined with RNA-Seq data, is presumptive evidence for SP9 *in vivo* binding and possible transcriptional regulation of a locus. E13.5 ChIP-Seq had 6272 peaks and E16.5 ChIP-Seq had 6561 peaks (Fig. 9A). Intersection of the two ChIP results yielded 3976 binding peaks (Fig. 9A, ∼60% overlap). SP9 binding was located in intergenic (∼36%), intronic (∼30%), promoter [±1 kb of the TSS (transcription start site)] (27%), and other genomic regions (exon, 5′ UTR and 3′ UTR) (Fig. 9B). *De novo* motif discovery using genomic sequences associated with SP9 binding was performed using HOMER (Heinz et al., 2010). The most frequent *de novo* motif, likely representing the primary sequence motif, enriched to the center of SP9-bound DNA fragments (Fig. 9D). According to the *de novo* motif analyses, (G|T)(G|C)TAATTA is the primary motif of SP9 in the developing ganglionic eminences (Fig. 9D), and ∼40% binding peaks had this motif. In addition to SP9 motifs, frequent motifs included in DLX1, YY2 and MEIS1 were also present in the SP9 ChIP-Seq peaks (Fig. 9E). The TF genes *Dlx1* and *Meis1* are highly expressed in the LGE (Long et al., 2009), suggesting that they may function as co-regulators with SP9 to promote striatal development.

We found an SP9 ChIP-Seq peak at the *Six3* promoter region (−5 to +411 of the TSS) (Fig. 9C), and several additional peaks upstream of the *Six3* gene (regions 1, 2 and 3) (Fig. 9C); each of these loci are evolutionarily conserved (see mammal conservation track in Fig. 9C). Thus, these noncoding domains are strong candidates for the *Six3* promoter and three *Six3* enhancers.

Next, to test the ability of SP9 to regulate these candidate regulatory elements, we performed a dual-luciferase transcription activation assay using P19 embryonal carcinoma cells. SP9 robustly activated transcription from the putative promoter of *Six3* and to a lesser extent from *Six3* region 1, whereas it did not activate *Six3* region 2 and 3 (Fig. 9F). Together, these results provide evidence that SP9 promotes *Six3* expression in the LGE SVZ through direct binding to the promoter and possibly through binding to regulatory elements within the *Six3* locus.

DISCUSSION

The dLGE mainly generates OB interneurons, whereas the vLGE mainly generates striatal MSNs. *Sp8-CKO* and *Sp9-KO* single mutants differentially alter LGE development. The salient phenotype of *Sp8-CKO* mice is disruption of OB interneuron development (Waclaw et al., 2006; Li et al., 2011, 2017), whereas in *Sp9-KO* mice D2-MSN development is disrupted (Zhang et al., 2016). Here, by comparing the phenotype of *Sp8/9-DCKO* with that of the single mutants, we provide evidence for distinct and

Development (2018) 145, dev165456. doi:10.1242/dev.165456

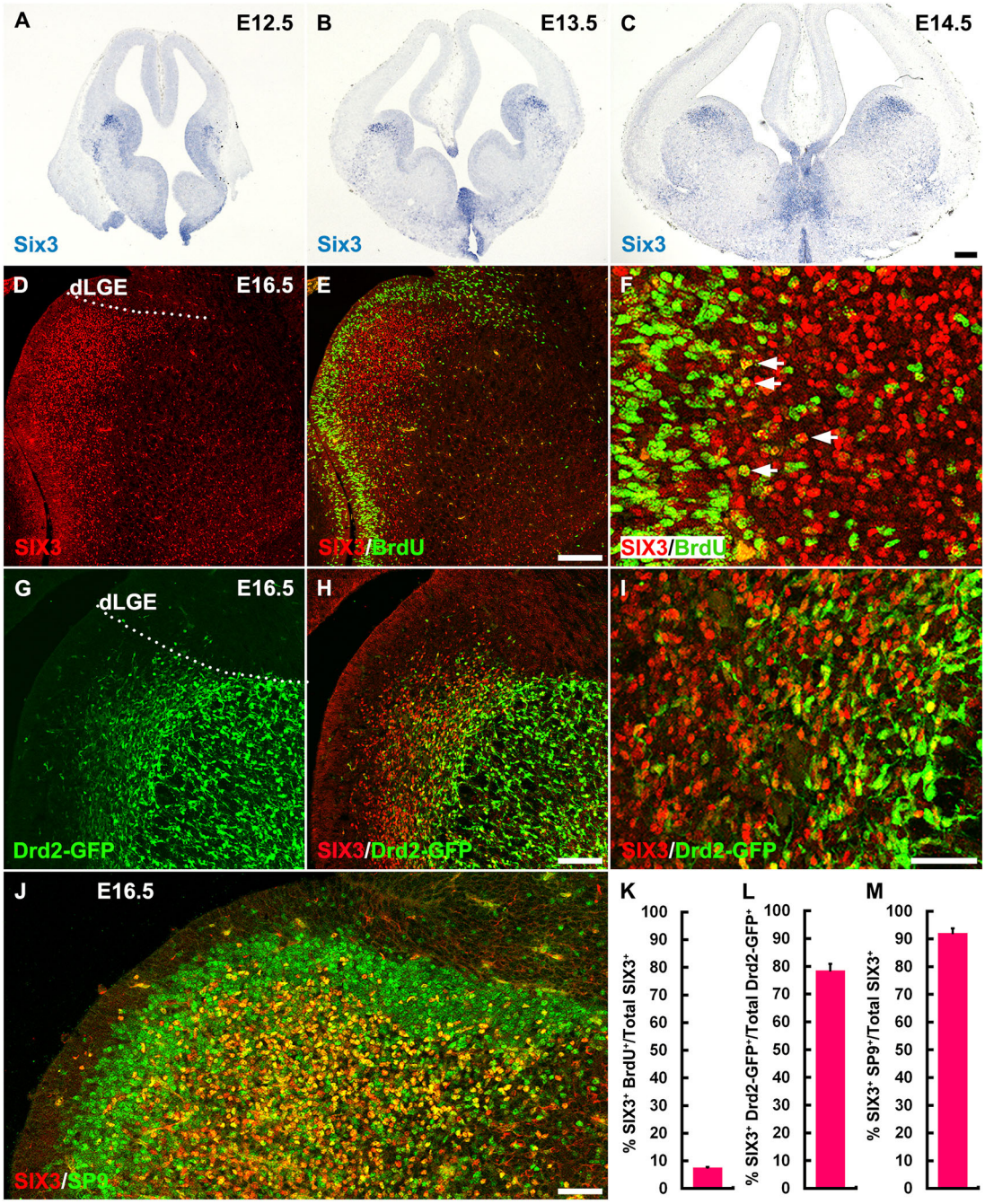

Fig. 6. *Six3* expression in the LGE. (A-C) *In situ* hybridization shows *Six3* expression in the ganglionic eminences, weak *Six3* expression in the VZ and strong *Six3* expression in the dorsal part of the vLGE SVZ. (D-F) Immunostaining of BrdU and SIX3 on LGE sections at E16.5, 30 min after a BrdU pulse. Arrows point to $BrdU^+/SIX3^+$ cells. Note that SIX3 expression was downregulated from the SVZ to the striatum. (G-J) Immunostaining of DRD2-GFP, SIX3 and SP9 on LGE sections at E16.5. The dLGE SVZ did not express SIX3. (K-M) Quantification of immunostaining experiments showing that, in the LGE SVZ, most $DRD2\text{-}GFP^+$ cells expressed SIX3 and most $SIX3^+$ cells expressed SP9. *n*=3, mean+s.e.m. Scale bars: 200 µm in C for A-C; 200 µm in D for D,E; 100 µm in H for G,H; 50 µm in I for F,I; 50 µm in J.

redundant functions of *Sp8* and *Sp9*. Our RNA-Seq and SP9 ChIP-Seq results provide strong evidence that *Sp8* and *Sp9* coordinately promote D2 MSN production by directly activating *Six3* transcription.

Sp8 and *Sp9* have some distinct functions in the LGE

Sp8 and *Sp9* expression are regionally distinct within the LGE. Strong *Sp8* expression is largely restricted to the SVZ of the dLGE (pLGE1 and 2), and weak *Sp8* expression is largely restricted to the SVZ of the vLGE (pLGE3). By contrast, *Sp9* is expressed uniformly throughout the SVZ of the LGE (pLGE1-4). The strongest effect of *Sp8* knockout is in the dLGE, whereas the strongest effect of *Sp9* knockout is in the vLGE. Although *Sp8* and *Sp9* have redundant functions in promoting neurogenesis in the OB (Li et al., 2017) and striatum (this study), they have different leading roles in these processes.

During OB interneuron development in the dLGE and postnatal SVZ-RMS-OB, *Sp8* has the central role, based on three lines of

Development (2018) 145, dev165456. doi:10.1242/dev.165456

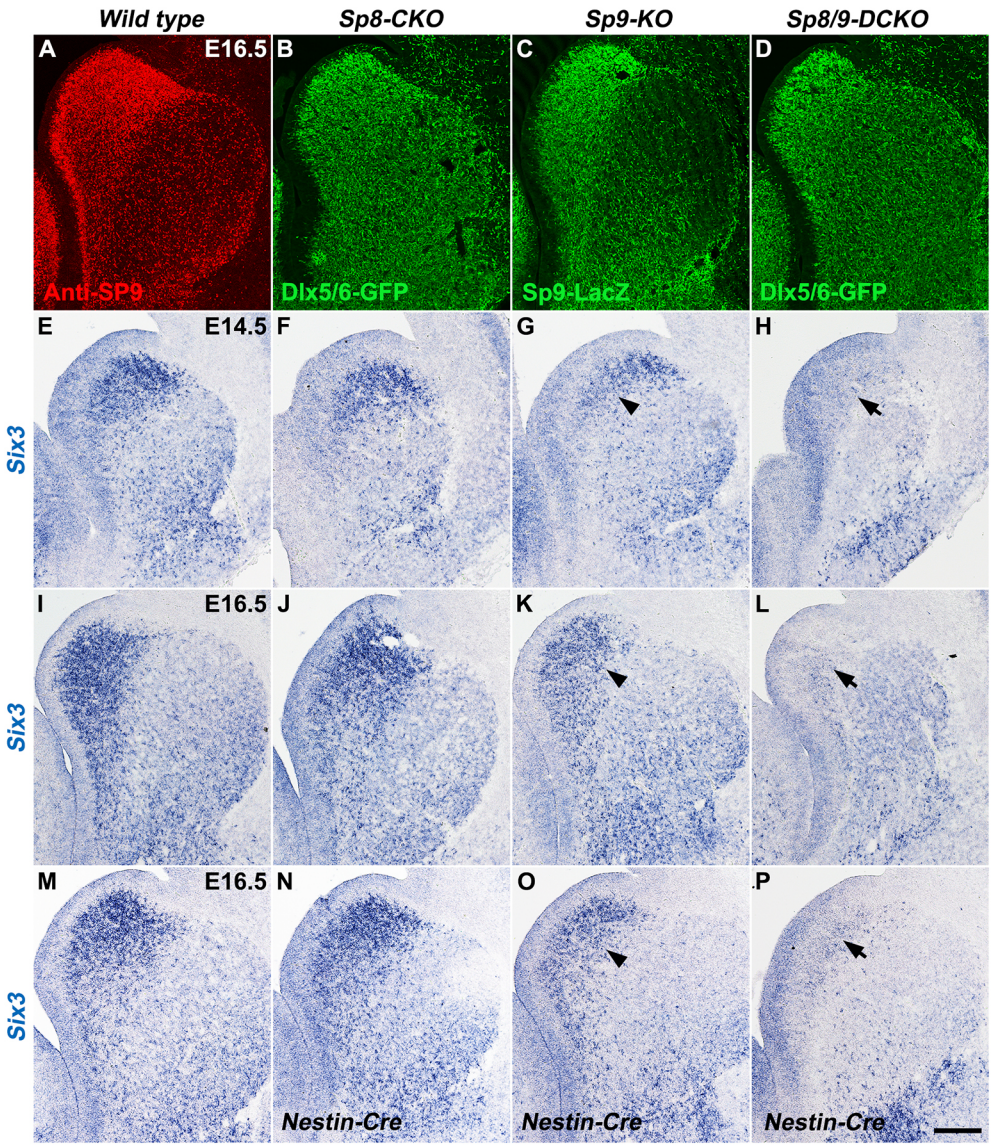

Fig. 7. *Sp8/9-DCKO* mice fail to express *Six3* in the LGE SVZ. (A-D) Immunostaining images show expressions of SP9, Dlx5/6-GFP, SP9-*lacZ* and Dlx5/6-GFP in the LGE of wild-type, *Sp8-CKO*, *Sp9-KO* and *Sp8/9-DCKO* mice, respectively. (E-L) *In situ* hybridization showing *Six3* expression in wild-type and mutant LGE at E14.5 and E16.5. *Six3* expression was reduced in the *Sp9-KO* LGE SVZ (arrowheads), and was almost undetectable in the *Sp8/9-DCKO* LGE SVZ (arrows), whereas *Six3* expression in the LGE of *Sp8-CKO* mice was less affected. (M-P) *Six3* expression in the LGE SVZ was also undetectable (P) when a *Nestin-Cre* transgenic allele was used to knockout *Sp8* and *Sp9*. Scale bar: 200 µm in P for A-P.

evidence. First, *Sp8* expression is upregulated in the *Sp9*-KO OB, whereas *Sp9* expression is not upregulated in the *Sp8-CKO* OB (Li et al., 2017). Second, a large number OB interneurons are depleted in *Sp8-CKO* mice (Waclaw et al., 2006; Li et al., 2011, 2017), but not in *Sp9-KO* mice (Li et al., 2017). Third, *Prokr2* and *Tshz1* expression levels are reduced in the dLGE and postnatal SVZ of *Sp8-CKO* mice, but not in *Sp9-KO* mice (Li et al., 2017). *Prokr2* and *Tshz1* are known to promote OB neuronal differentiation and migration and are involved in human Kallmann syndrome (Ng et al., 2005; Matsumoto et al., 2006; Ragancokova et al., 2014).

Sp8 is required to promote neuronal differentiation (transition of neural progenitors to neurons) in the SVZ of the LGE. Loss of *Sp8* function results in subtle accumulation of neural progenitors in both the dLGE and the vLGE (Fig. 4, Fig. S6). In contrast, accumulation of neural progenitors is not observed in *Sp9* mutant LGE SVZ (Fig. 4, Fig. S6).

During the generation of D2 MSNs in the vLGE, *Sp9* has the central role, based on four lines of evidence. First, in the SVZ of the vLGE, *Sp9* is strongly expressed, whereas *Sp8* is weakly expressed (Fig. 1, Figs S1 and S2). Second, unlike *Sp8*, which is downregulated in most D2 MSNs, *Sp9* is expressed in nearly all postmitotic D2 MSNs and promotes their differentiation and survival (Fig. S1E-H) (Zhang et al., 2016). Third, there are many more MSNs, especially D2 MSNs, lost in *Sp9-KO* mice than in *Sp8-CKO* mice. Fourth, *Six3* expression in the LGE SVZ is downregulated in *Sp9-KO*, but not in *Sp8-CKO*, mice (Fig. 7, Fig. S10).

Redundant functions of *Sp8* and *Sp9* in the LGE

In *Sp9* mutants, *Sp8* expression is more broadly expressed in the SVZ (Fig. 1I,J and Fig. S2), suggesting that this may enable to *Sp8* compensate for the loss of *Sp9*. Indeed, this hypothesis is borne out. In the *Sp8/9-DCKO*, development of both OB interneurons and striatal D2 MSNs are much more severely disrupted than in single mutants (Li et al., 2017) (Fig. 3, this study). *Sp8* also compensates in striatal development of *Sp9-KO* mice, in which the few D2 MSNs that are produced have increased SP8 expression (Fig. 2C-N).

As noted above, *Sp8-CKO* mice have more progenitors in the LGE than do controls and *Sp9-CKO* mice (Fig. 4, Fig. S6). Furthermore, in the *Sp8/9-DCKO* mice there are more VZ-SVZ

Development (2018) 145, dev165456. doi:10.1242/dev.165456

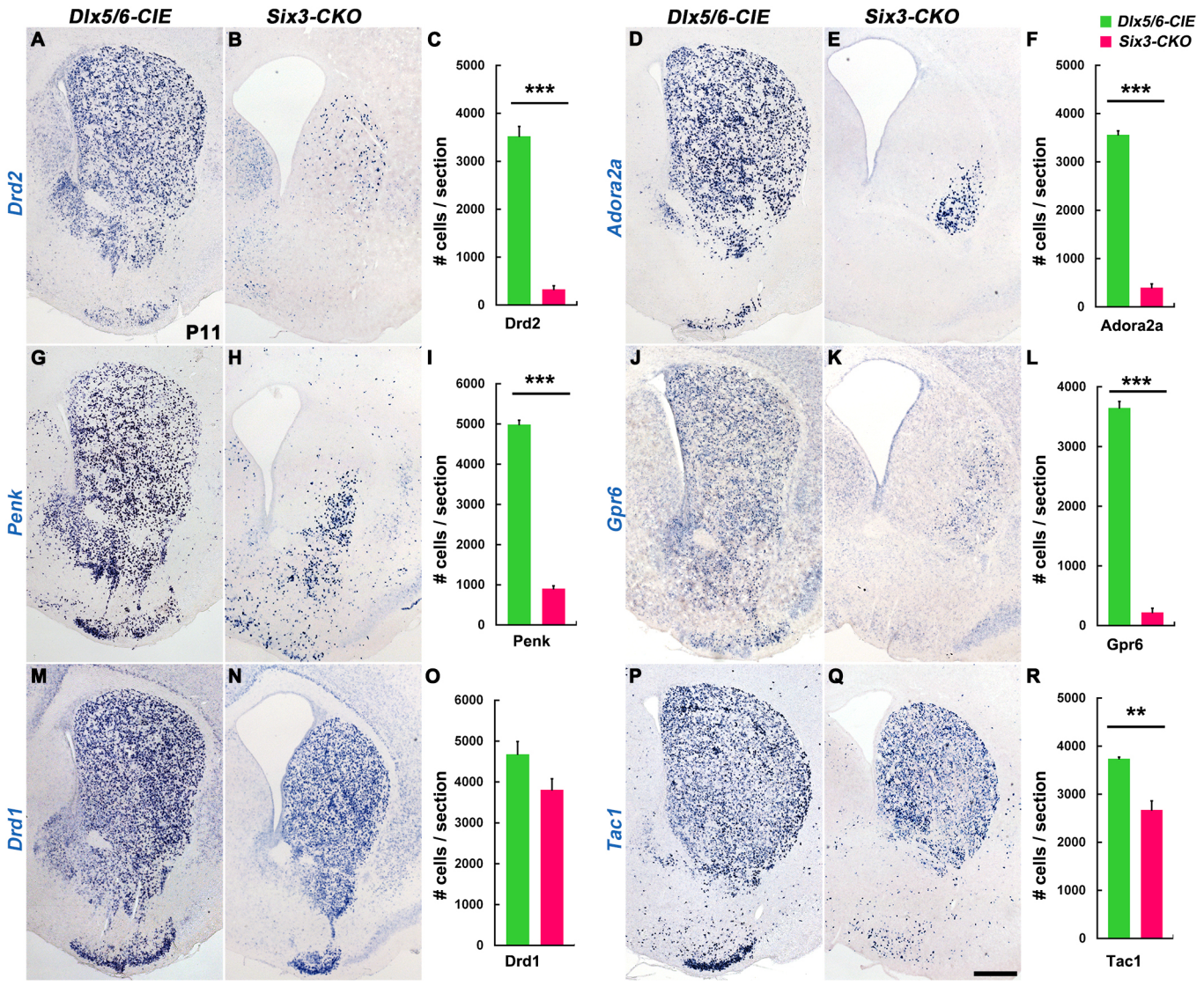

Fig. 8. Most D2 MSNs were lost in the striatum of *Six3-CKO* mice. (A-L) *In situ* RNA hybridization of *Drd2*, *Adora2a*, *Penk* and *Gpr6* showing that >90% of D2 MSNs were lost in the striatum of *Six3-CKO* mice compared with controls (*Dlx5/6-CIE*) at P11. (M-R) The generation of D1 MSNs (*Drd1*$^+$ and *Tac1*$^+$ cells) was less affected. Note that the lateral ventricle was enlarged in *Six3-CKO* mice. (Student's *t*-test, ***P*<0.01, ****P*<0.001, *n*=3, mean+s.e.m.). Scale bar: 500 µm in Q for A-Q.

progenitors than in *Sp8-CKO* mice (Fig. 4, Fig. S6). Thus, together *Sp8* and *Sp9* promote the progression of progenitors out of the cell cycle and towards a neural fate.

In the *Sp8/9-DCKO* mice, newly born neuroblasts in the dLGE and postnatal SVZ-RMS-OB fail to express *Prokr2* and *Tshz1* lack virtually all OB mature interneurons. We suggest that the lack of *Prokr2* and *Tshz1* RNA in large part accounts for the defects in differentiation and migration (tangential and radial) of OB immature interneurons, as similar phenotypes are observed in *Prokr2* (and *Tshz1*) mutant mice (Ng et al., 2005; Matsumoto et al., 2006; Ragancokova et al., 2014; Li et al., 2017). Thus, in the dLGE and postnatal SVZ-RMS, *Sp8* and *Sp9* coordinately regulate OB interneuron development mainly by promoting *Prokr2* and *Tshz1* expression; however, here *Sp8* has the leading role. This contrasts with the vLGE, where *Sp9* has the leading role in driving *Six3* expression and the generation of D2 MSNs (Fig. 7) (Zhang et al., 2016). Nonetheless, *Sp8* can compensate in this process as well.

Loss of *Sp8/9* function disrupts LGE progenitors

In *Sp8/9-DCKO* mutants, neural progenitors accumulate in the SVZ (Fig. 4, Fig. S6) (Li et al., 2017). These cells have increased *Dlx1/2* TF expression (Fig. 4, Fig. S6), which provides evidence that they are arrested as immature neural progenitors (Yun et al., 2002). A subset of mutant SVZ cells have also increased ASCL1$^+$ proneural TF expression. ASCL1, by driving *Dll1* (delta-like 1) expression, can increase Notch signaling in adjacent cells and thereby promote the maintenance of their progenitor state (Fig. 4, Fig. S6, Table S1) (Castro et al., 2011). In addition, ASCL1 promotes expression of genes that inhibit cell cycle progression and/or promote cell cycle arrest (Fig. 4, Fig. S6) (Castro et al., 2011).

Sp8 and *Sp9* have minor roles in D1 MSN development

In the striatum, we observed that D1 MSNs were largely unaffected in *Sp8-CKO*, *Sp9-KO* and *Sp8/9-DCKO* mice (Fig. 3K-T, Fig. S5Q-X). In addition, we observed a reduced number of EBF1$^+$ cells in the LGE SVZ of *Sp8/9-DCKO* mice at E16.5 (Fig. 5F-J). The TF *Ebf1*

Development (2018) 145, dev165456. doi:10.1242/dev.165456

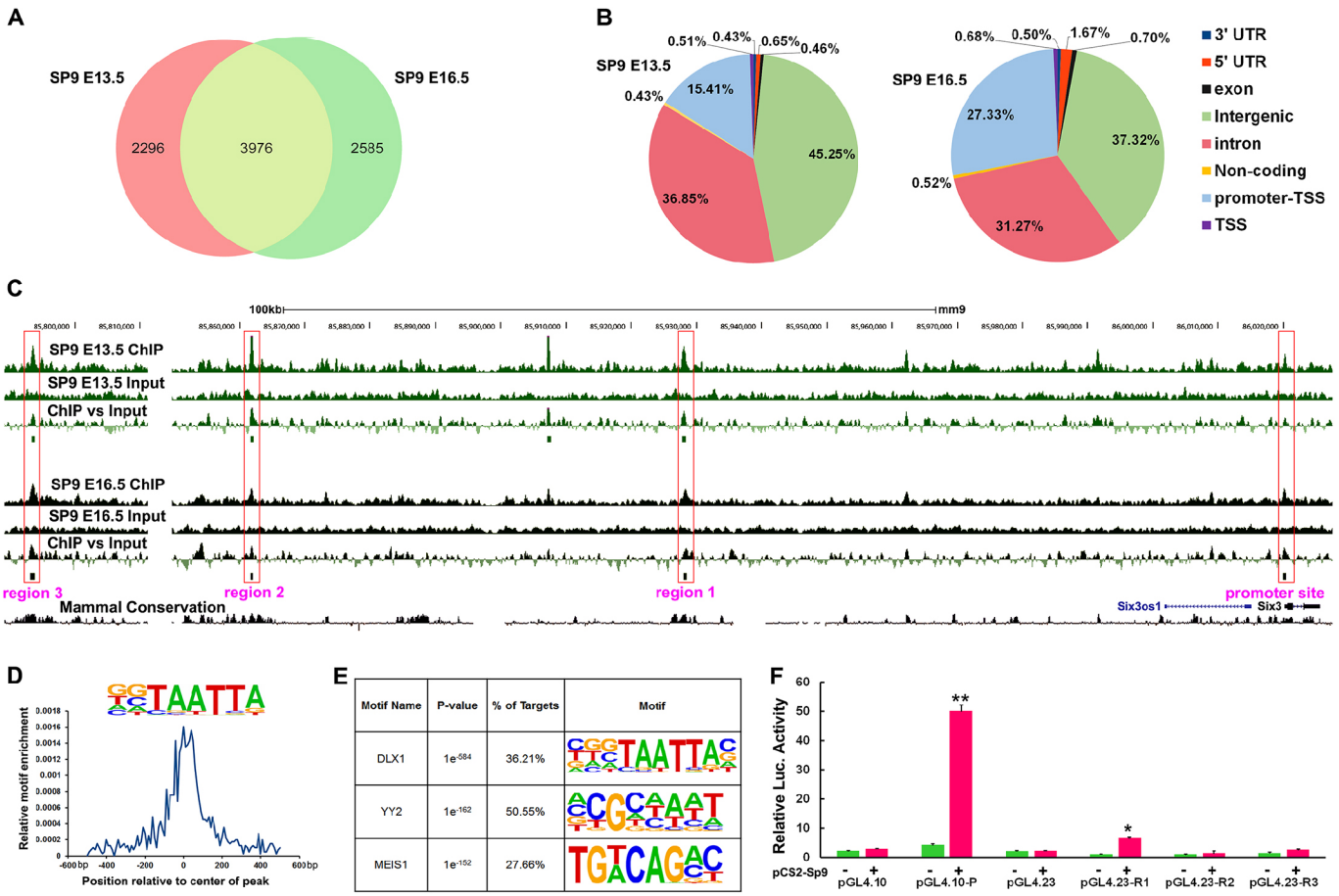

Fig. 9. SP9 binds to the promoter of *Six3*. (A) Venn diagram showing overlap of called peaks between SP9 ChIP at E13.5 and E16.5. (B) Pie charts showing genomic distribution of SP9-binding peaks (for E13.5 and E16.5 experiments) relative to promoters (within ±1 kb of TSS), 5′ UTRs, exons, introns, 3′ UTRs and intergenic regions. (C) ChIP-Seq genome browser tracks from E13.5 (green) and E16.5 (black) experiments, showing SP9 ChIP, input and ChIP versus input. Small rectangles beneath the tracks indicate called peaks. Large red rectangles highlight where SP9 binds to the promoter and several upstream regions (regions 1, 2 and 3) of the *Six3* gene. (D) SP9 consensus motif and relative enrichment derived from *de novo* motif analysis of intersected SP9 ChIP-Seq. (E) Top three frequent motifs (according to *P*-value) derived from the intersection of two ChIP experiments, displaying the associated transcription factor and percentage of total peaks. (F) SP9-activated transcription from the *Six3* promoter and a putative enhancer in a dual-luciferase assay within P19 cells. P, promoter; R1, region 1; R2, region 2; R3, region 3. Student's *t*-test, **P*<0.05, ***P*<0.01, *n*=3 individuals, mean+s.e.m.

is specifically expressed in young D1 MSNs, and is essential for the differentiation of D1 MSNs (Lobo et al., 2006, 2008). Thus, reduced EBF1^{+} cells in the LGE SVZ provides evidence that SVZ cells in the D1 MSN developmental pathway may not be normal. However, this could be a result of a general SVZ phenotype in the mutants as the increased ASCL1 expression is observed in the presumptive both D1 and D2 MSN progenitors. Therefore, EBF1 reduction in the E16.5 LGE SVZ does not directly demonstrate a defect in the development of D1 MSNs.

Function of *Six3* in the generation of D2 MSNs

Six3 has multiple roles in embryonic development. In the forebrain, *Six3* is required to activate SHH signaling and repress WNT signaling to provide key patterning instructions (Lagutin et al., 2003; Geng et al., 2008). In retinal development, *Six3* is crucial for the activation of *Pax6*, a key regulator of eye development (Liu et al., 2006). *Six3* is also required for ependymal cell maturation; *Six3* mutants develop hydrocephaly (Lavado and Oliver, 2011).

Six3 is expressed in the developing basal ganglia. Mice haploinsufficient for *Six3* (*Six3*$^{+/ki}$; *Shh*$^{+/-}$ mouse) fail to activate *Shh* and *Nkx2-1* expression in the MGE (Geng et al., 2008; Geng and Oliver, 2009), whereas *Ebf1* expression in the LGE is largely unaffected. A recent study (Gokce et al., 2016) and our analysis indicate that during striatal development *Six3* is preferentially expressed in and functions in the D2 MSN lineage (Figs 6 and 8), but not in the D1 MSN lineage (Fig. S9). Furthermore, *Sp9* and *Sp8/9* mutants have greatly reduced *Six3* expression (Fig. 7, Fig. S10), and *Six3-CKO* mutants fail to generate most D2 MSNs, which closely phenocopies the *Sp8/9-DCKO* mutants (Fig. 3, Fig. S3, Fig. 8).

Six3 is not expressed in the dLGE (Fig. 6, Fig. S8) and, accordingly, the *Six3-CKO* mutants did not show altered *Tshz1* expression in the dLGE (Fig. S11). *Six3* is also not expressed in the postnatal SVZ-RMS-OB (data not shown and Allen Developing Mouse Brain Atlas: developingmouse.brain-map.org/gene/show/20235). Thus, it is not surprising that we did not find major olfactory bulb interneuron defects in the *Six3-CKO* mice (data not shown). *Six3* LGE expression is restricted to the vLGE SVZ, and is most prominent in the pLGE3 (Flames et al., 2007). This suggests that D2 MSNs are largely generated by pLGE3. We hypothesize that D1 MSNs are mainly generated by a more ventral domain (pLGE4). Future studies should address this hypothesis and also search for additional transcription mechanisms that generate D1 MSNs (Lobo et al., 2006; Shirasaki et al., 2012; Ehrman et al., 2013; Lu et al., 2014; Merchan-Sala et al., 2017).

Development (2018) 145, dev165456. doi:10.1242/dev.165456

To investigate the genomic loci regulated by SP9, we performed SP9 ChIP-seq using E13.5 and E16.5 ganglionic eminences. We found that SP9 binds to the *Six3* promoter and several putative *Six3* enhancers. The *Six3* promoter was strongly activated by SP9 in luciferase reporter assays. In addition, one putative enhancer (*Six3* region 1, Fig. 9C) was moderately activated. Thus, we propose that SP9 directly promotes *Six3* expression in the pLGE3 SVZ.

In summary, this study provides evidence that *Sp8/9* and *Six3* are crucial components in the SVZ of the pLGE3, where they selectively drive the generation of D2 MSNs. Thus, these findings broaden the foundation for elucidating the transcriptional mechanisms underlying striatal MSN development and survival. This information has ramifications for understanding how to engineer MSNs *in vitro*, and for understanding disorders of striatal development and degeneration.

MATERIALS AND METHODS

Animals

All experiments were performed in accordance with institutional guidelines at Fudan University. $Sp9^{lacZ/+}$ (Zhang et al., 2016), $Sp9^{F/F}$ (Zhang et al., 2016), $Sp8^{F/F}$ (Bell et al., 2003), $Six3^{F/F}$ (Liu et al., 2006), $Bax^{-/+}$ (Knudson et al., 1995), *Dlx5/6-CIE* (Stenman et al., 2003), *Nestin-Cre* (Tronche et al., 1999; Graus-Porta et al., 2001) and *Drd2-GFP* (from MMRRC) (Gong et al., 2007) mice were previously described. Wild-type, *Dlx5/6-CIE* or *Sp8/9* floxed littermate mice without Cre allele were used as controls. Mice were group-housed with approximately four to a cage on a 12-h light, 12-h dark cycle, with *ad libitum* chow and water. These mice were maintained in a mixed genetic background of C57BL/6J, 129S6 and CD1. The day of vaginal plug detection was calculated as E0.5, and the day of birth was considered as P0. Males and females were both used in all experiments.

BrdU labeling

A single intraperitoneal injection of BrdU (50 mg/kg, body weight) was given to pregnant dams at E13.5, and the pups were sacrificed at P0, or a single intraperitoneal injection of BrdU was given to pregnant dams at E15.5, and the mice were sacrificed at E16.5.

Immunohistochemistry

Postnatal mice were deeply anesthetized and perfused intracardially with 4% paraformaldehyde (PFA) in 1×PBS (pH 7.4); embryonic brains were fixed by immersion in 4% PFA. All brains were fixed overnight in 4% PFA, cryoprotected in 30% sucrose for at least 24 h, frozen in embedding medium and cryosectioned.

Immunohistochemistry was performed on 12-µm-thick cryostat sections on Fisherbrand Superfrost Plus microscope slides or 30- to 50-µm-thick free-floating sections (Ma et al., 2013; Zhang et al., 2016). For SP9, EBF and SIX3 immunohistochemistry, sections were boiled in 10 mM sodium citrate briefly for antigen retrieval (Ma et al., 2013). For BrdU staining, sections were incubated in 2 N HCl for 1 h at room temperature, and then rinsed in 0.1 M borate buffer twice (Liu et al., 2009).

The following primary antibodies were used: rabbit anti-SP9 (1:500) (Zhang et al., 2016), goat anti-SP8 (1:3000; Santa Cruz Biotechnology, sc-104661); chicken anti-GFP (1:3000; Aves Labs, GFP-1020); rabbit anti-ASCL1 (1:2000; Cosmo Bio, SK-T01-003); rat anti-BCL11b (1:2000; Abcam, ab18465); rat anti-BrdU (1:200, Accurate Chemical, OBT0030s); chicken anti-β-gal (1:1000; Abcam, ab9361); rabbit anti-cleaved caspase 3 (1:300; Cell Signaling, 9661); rabbit anti-FOXP1 (1:2000; Abcam, ab16645); goat anti-DCX (1:1000; Santa Cruz Biotechnology, sc-8066); mouse anti-TUBB3 (1:500; Covance, MMS-435P); goat anti-EBF (1:200; Santa Cruz Biotechnology, sc-15888); rabbit anti-EBF1 (1:2000; Merck, AB10523); mouse anti-SIX3 (1:500; Santa Cruz Biotechnology, sc-398797); rabbit anti-SIX3 (1:2000; Rockland Immunochemicals, 600-401-A26).

In situ RNA hybridization

All *in situ* RNA hybridization experiments were performed using digoxigenin-labeled riboprobes on 20-µm-thick cryostat sections (Long et al., 2009; Zhang et al., 2016). Riboprobes were amplified by PCR using the following primers: *Gsx2* Forward: CCTTTGTTCGAGTCCCAGACACC; *Gsx2* Reverse: AAAGGGACTTCCAGAGACCTGGAT; *Dlx1* Forward: ATGACCATGACCACCATGCCAG; *Dlx1* Reverse: TCACATCAGTTGAGGCTGCTGC; *Dlx2* Forward: TTTCCTGTCCCGGGTCAGGAT; *Dlx2* Reverse: AAGTCTCAGACGCTGTCCACTCGA; *Ascl1* Forward: CTAACAGGCAGGGCTGGA; *Ascl1* Reverse: TAAGGGGTGGGTGTGAGG; *Hes5* Forward: TAATCGCCTCCAGAGCTCCAGGC; *Hes5* Reverse: ACACAAAACAACCCCACGGGGTC; *E2f1* Forward: TGGTAAGCGGCTTGAAGGCCTG; *E2f1* Reverse: AATGTGGCAGCAACCAAACCCC; *Cdca7* Forward: AGACTCTCGAGACGTTTGCTA; *Cdca7* Reverse: AGCTGCAGTTGCAAATTCCTC; *Cdk1* Forward: GATGTAGCCCTCTGGATGGA; *Cdk1* Reverse: GCCCCTGATCTCTAGCTGTG; *Gadd45g* Forward: CCCTCCGCACTCTTTTGGATAACT; *Gadd45g* Reverse: ATTCAAAGCTTCCACGATAGCGTC; *Btg2* Forward: GCCAGACCGTCATCATCGTTCTAAT; *Btg2* Reverse: CCTAGGCAAACACTGGCTCACAGA; *Six3* Forward: CTCTATTCCTCCCACTTCTTGTTGC; *Six3* Reverse: CATCACATTCCGAGTCGCTGG; *Chat* Forward: GATGCCTATCCTGGAAAAGGTCC; *Chat* Reverse: CGTTGGACGCC ATTTTGACTATC.

RNA-Seq

RNA-Seq analysis was performed as previously described (Li et al., 2017). The LGE (including VZ, SVZ and MZ) from E16.5 *Sp8/9-DCKO* mice and littermate controls (*Sp8/9* floxed mice without *Dlx5/6-CIE*) were dissected (n=3 mice per group). RNA quality was assessed using a bioanalyzer (Agilent Technologies). RNA-Seq libraries were prepared according to the Illumina TruSeq protocol. Levels of gene expression were reported in FPKM (Trapnell et al., 2012; Li et al., 2017). A gene was considered to be expressed if it had an FPKM>1. Genes were considered differentially expressed if P<0.05.

ChIP-Seq

SP9 ChIP-Seq was performed using dissected E13.5 and E16.5 ganglionic eminences (LGE+MGE) of wild-type CD1 mice, and an SP9 rabbit polyclonal antibody as described previously (McKenna et al., 2011; Sandberg et al., 2016; Zhang et al., 2016). Briefly, the E13.5 or E16.5 ganglionic eminences (including VZ, SVZ and MZ) (two litters for one independent ChIP experiment) were dissected, and fixed in 10 ml 1% formaldehyde for 10 min at room temperature. The formaldehyde was quenched by adding glycine to a final concentration of 0.125 M, and the samples were incubated for 5 min at room temperature. Tissues were then washed twice in cold PBS, pelleted, re-suspended in 1% SDS lysis buffer (with 1 mM PMSF/cocktail), and incubated on ice for 10 min. Sonication was performed using Bioruptor Pico (15-20 cycles) to keep most DNA fragments in the range of 200-500 bp. Eight micrograms anti-SP9 rabbit polyclonal antibody were incubated with the cleared chromatin (SDS concentration diluted to 0.1%) at 4°C overnight. Protein A+G beads were added to the samples and incubated for 4 h at 4°C. The samples were washed with low salt [150 mM NaCl, 0.1% w/v SDS, 1% Triton X-100, 2 mM EDTA, 20 mM Tris-HCl (pH 8.0)], high salt [500 mM NaCl, 0.1% w/v SDS, 1% Triton X-100, 2 mM EDTA, 20 mM Tris-HCl (pH 8.0)] and LiCl solutions [250 mM LiCl, 1% NP-40, 1% w/v sodium deoxycholate, 10 mM Tris-HCl (pH 8.0), 1 mM EDTA], and the precipitated DNA was eluted in elution buffer (0.1 M $NaHCO_3$ and 1% w/v SDS). The eluted DNA samples were reverse cross-linked overnight in the presence of 250 mM NaCl, treated with RNase and proteinase K and purified using the Zymo Research D5205 Kit. ChIP-seq sequencing libraries were prepared from both the input DNA and the precipitated DNA using the NEBNext DNA Library Prep Kit and Illumina standard adaptors, and were sequenced using a 150 bp pair-end strategy using the Illumina Hiseq 4000 platform.

Reads from the ChIP and input libraries were mapped to the mouse genome (mm9) using Bowtie with default parameters. Peak calling between the replicate ChIP samples and the input control sample was carried out using model-based analysis for ChIP-Seq (MACS). Peaks were called considering input as the control sample with filtering to remove peaks in repeat regions. Motif analysis of ChIP-Seq peak DNA sequences was performed using HOMER. ChIP-Seq peaks were visualized using the UCSC genome browser.

Development (2018) 145, dev165456. doi:10.1242/dev.165456

Luciferase assays

The DNA fragments of *Six3* promoter, *Six3* putative enhancers (region 1, region 2 and region 3, Fig. 9C) were amplified by PCR and subsequent cloned into pGL4.10 and pGL4.23 firefly luciferase vector (Promega) upstream of the *Luc2* gene, respectively (McKinsey et al., 2013).

The primers used for amplifying the *Six3* promoter were: Fwd: 5′-CCTCCGGCTAAGTGGTAAAACCGTC-3′; Rev: 5′-GGAGGAGGAAGGACGTAAGGGACAC-3′. The primers used for amplifying the *Six3* putative enhancers were: Region 1 Fwd: 5′-TATTGTTCGGGATTTGCCGAAATC-3′; Region 1 Rev: 5′-GAGGAGGCTGCCACTGCTTAACAG-3′; Region 2 Fwd: 5′-TAGGCGATTCAATAGTTAATGGAGG-3′; Region 2 Rev: 5′-ATGACAAACTCATCTCCCAGCATT-3′; Region 3 Fwd: 5′-CCAGGCCTCGCACAGTCTTTCTT-3′; Region 3 Rev: 5′-GAGCAGGGCAAACAATGAGCAAAC-3′. The coding sequence (CDS) of *Sp9* was amplified by PCR from mouse genomic DNA and cloned into pCS2 (+) expression vector, using the following primers: *Sp9* CDS Fwd: 5′-GACCTGAATCGTGATTCCCAGC-3′; *Sp9* CDS Rev: 5′-TGCAACCCACATAAACTTCATTGC-3′.

Mouse embryonal carcinoma P19 cells were grown in MEMα (Gibco, 12571-063) supplemented with 10% fetal bovine serum (Gibco 10099-141). For the luciferase assay, P19 cell transfections were performed in triplicate in 24-well plates using Fugene HD transfection reagent according to the manufacturer's protocol (Promega, E2311). The amounts of plasmids for each transfection were: 40 ng pGL4.73 (Promega, *Renilla* luciferase vector), 240 ng pCS2-empty or pCS2-*Sp9*, 240 ng pGL4.23-empty (pGL4.10-empty) (Promega), or pGL4.23-Element (pGL4.10-Promoter). The dual luciferase assay was performed with a GloMax 20/20 Luminometer (Promega). Statistical significance was determined by Student's *t*-test.

Microscopy

Bright-field images (*in situ* hybridization results) and some fluorescent images were imaged with Olympus BX 51 microscope using a 4× or 10× objective. Other fluorescent images were taken with the Olympus FV1000 confocal microscope system using 10×, 20×, 40× or 60× objectives. *z*-stack confocal images were reconstructed using FV10-ASW software. All images were merged, cropped and optimized in Photoshop CS5 without distortion of the original information.

Quantification

Cell quantification was made in the SVZ of LGE or in the striatum using three randomly chosen sections from mutant and their respective control mice (n=3 mice per genotype per age).

The numbers of DRD2-GFP$^+$/SP8$^+$ cells in the striatum of *Drd2-GFP* control and *Drd2-GFP; Sp9-KO* mice at P9 were quantified in three randomly chosen 30-µm-thick sections from each mouse, and three mice each group were analyzed.

The numbers of *Drd2*$^+$, *Adora2a*$^+$, *Drd1*$^+$, *Tac1*$^+$ and *ChAT*$^+$ cells in the striatum of *Dlx5/6-CIE* control, *Sp8-CKO*, *Sp9-KO*, *Sp8/9-DCKO* and *Six3-CKO* mice at P11 were quantified in three randomly chosen 20-µm-thick sections from each mouse, and three mice per group were analyzed.

The LGE VZ and SVZ were defined based on a BrdU pulse-labeling experiment (see Fig. S1E-H). The numbers of FOXP1$^+$ and EBF1$^+$ cells in the E16.5 LGE SVZ, the numbers of BrdU$^+$ cells in the LGE VZ/SVZ and MZ, and the numbers of BrdU$^+$ cells in the P0 striatum were quantified in three randomly chosen 12-µm-thick sections from each mouse, and three mice per group were analyzed.

The numbers of cleaved caspase 3$^+$ cells in the P0, P2 and P3 striatum were quantified in three randomly chosen 20-µm-thick sections from each mouse, and three mice per group were analyzed.

The numbers of SIX3$^+$, SIX3$^+$/BrdU$^+$, DRD2-GFP$^+$ and SIX3$^+$/DRD2-GFP$^+$ cells in the E16.5 LGE SVZ were quantified in three randomly chosen 12-µm-thick sections from each mouse, and three mice per group were analyzed.

Statistics

Statistical significance was assessed using unpaired Student's *t*-test or one-way ANOVA followed by the Tukey–Kramer post-hoc test. All quantification results were presented as the mean+s.e.m. *P*-values less than 0.05 were considered significant.

Acknowledgements

We are grateful to Guillermo Oliver at Northwestern University for the generous gift of *Six3*$^{F/F}$ mice, and Kenneth Campbell at University of Cincinnati College of Medicine for the *Sp8*$^{F/F}$ and Dlx5/6-CIE mice.

Competing interests

J.L.R. is a co-founder and stockholder, and is currently on the scientific board, of Neurona, a company studying the potential therapeutic use of interneuron transplantation.

Author contributions

Conceptualization: B.C., J.L.R., Z.Y.; Methodology: Z.X., Q.L., X.S., Z.Z., S.L., Z.L., Y.W., G.L., T.G., D.Q., M.W., C.W.; Software: H.F.; Formal analysis: Z.X., Q.L., X.S.; Data curation: Z.X., Q.L., X.S., X.W.; Writing - original draft: Z.Y.; Writing - review & editing: B.C., J.L.R., Z.Y.; Visualization: Z.X., Q.L., X.S.; Supervision: H.L.; Project administration: Y.Y., Z.Y.; Funding acquisition: Z.Y.

Funding

This work was supported by grants from National Natural Science Foundation of China (31630032, 31425011, 31421091 and 31429002 to Z.Y.; 31722099 to Y.Y.; 81500977 to D.Q.) and from the National Institutes of Health (MH094589 and NS089777 to B.C.; MH049428 to J.L.R.). Deposited in PMC for release after 12 months.

Data availability

RNA-Seq and ChIP-Seq data have been deposited in Gene Expression Omnibus under accession number GSE114344. These data have also been deposited at NODE, accession number OEP000035.

Supplementary information

Supplementary information available online at
http://dev.biologists.org/lookup/doi/10.1242/dev.165456.supplemental

References

Appolloni, I., Calzolari, F., Corte, G., Perris, R. and Malatesta, P. (2008). Six3 controls the neural progenitor status in the murine CNS. *Cereb. Cortex* **18**, 553-562.

Bell, S. M., Schreiner, C. M., Waclaw, R. R., Campbell, K., Potter, S. S. and Scott, W. J. (2003). Sp8 is crucial for limb outgrowth and neuropore closure. *Proc. Natl. Acad. Sci. USA* **100**, 12195-12200.

Castro, D. S., Martynoga, B., Parras, C., Ramesh, V., Pacary, E., Johnston, C., Drechsel, D., Lebel-Potter, M., Garcia, L. G., Hunt, C. et al. (2011). A novel function of the proneural factor Ascl1 in progenitor proliferation identified by genome-wide characterization of its targets. *Genes Dev.* **25**, 930-945.

Del Bene, F. and Wittbrodt, J. (2005). Cell cycle control by homeobox genes in development and disease. *Semin. Cell Dev. Biol.* **16**, 449-460.

Del Bene, F., Tessmar-Raible, K. and Wittbrodt, J. (2004). Direct interaction of geminin and Six3 in eye development. *Nature* **427**, 745-749.

Durieux, P. F., Bearzatto, B., Guiducci, S., Buch, T., Waisman, A., Zoli, M., Schiffmann, S. N. and de Kerchove d'Exaerde, A. (2009). D2R striatopallidal neurons inhibit both locomotor and drug reward processes. *Nat. Neurosci.* **12**, 393-395.

Ehrman, L. A., Mu, X., Waclaw, R. R., Yoshida, Y., Vorhees, C. V., Klein, W. H. and Campbell, K. (2013). The LIM homeobox gene Isl1 is required for the correct development of the striatonigral pathway in the mouse. *Proc. Natl. Acad. Sci. USA* **110**, E4026-E4035.

Ena, S. L., De Backer, J.-F., Schiffmann, S. N. and de Kerchove d'Exaerde, A. (2013). FACS array profiling identifies Ecto-5′ nucleotidase as a striatopallidal neuron-specific gene involved in striatal-dependent learning. *J. Neurosci.* **33**, 8794-8809.

Flames, N., Pla, R., Gelman, D. M., Rubenstein, J. L. R., Puelles, L. and Marin, O. (2007). Delineation of multiple subpallial progenitor domains by the combinatorial expression of transcriptional codes. *J. Neurosci.* **27**, 9682-9695.

Geng, X. and Oliver, G. (2009). Pathogenesis of holoprosencephaly. *J. Clin. Invest.* **119**, 1403-1413.

Geng, X., Speirs, C., Lagutin, O., Inbal, A., Liu, W., Solnica-Krezel, L., Jeong, Y., Epstein, D. J. and Oliver, G. (2008). Haploinsufficiency of Six3 fails to activate Sonic hedgehog expression in the ventral forebrain and causes holoprosencephaly. *Dev. Cell* **15**, 236-247.

Gerfen, C. R. and Surmeier, D. J. (2011). Modulation of striatal projection systems by dopamine. *Annu. Rev. Neurosci.* **34**, 441-466.

Gokce, O., Stanley, G. M., Treutlein, B., Neff, N. F., Camp, J. G., Malenka, R. C., Rothwell, P. E., Fuccillo, M. V., Südhof, T. C. and Quake, S. R. (2016). Cellular

taxonomy of the mouse striatum as revealed by single-cell RNA-seq. *Cell Rep.* **16**, 1126-1137.

Gong, S., Doughty, M., Harbaugh, C. R., Cummins, A., Hatten, M. E., Heintz, N. and Gerfen, C. R. (2007). Targeting Cre recombinase to specific neuron populations with bacterial artificial chromosome constructs. *J. Neurosci.* **27**, 9817-9823.

Graus-Porta, D., Blaess, S., Senften, M., Littlewood-Evans, A., Damsky, C., Huang, Z., Orban, P., Klein, R., Schittny, J. C. and Müller, U. (2001). Beta1-class integrins regulate the development of laminae and folia in the cerebral and cerebellar cortex. *Neuron* **31**, 367-379.

Heiman, M., Schaefer, A., Gong, S., Peterson, J. D., Day, M., Ramsey, K. E., Suárez-Fariñas, M., Schwarz, C., Stephan, D. A., Surmeier, D. J. et al. (2008). A translational profiling approach for the molecular characterization of CNS cell types. *Cell* **135**, 738-748.

Heinz, S., Benner, C., Spann, N., Bertolino, E., Lin, Y. C., Laslo, P., Cheng, J. X., Murre, C., Singh, H. and Glass, C. K. (2010). Simple combinations of lineage-determining transcription factors prime cis-regulatory elements required for macrophage and B cell identities. *Mol. Cell* **38**, 576-589.

Knudson, C. M., Tung, K. S. K., Tourtellotte, W. G., Brown, G. A. J. and Korsmeyer, S. J. (1995). Bax-deficient mice with lymphoid hyperplasia and male germ cell death. *Science* **270**, 96-99.

Kobayashi, M., Toyama, R., Takeda, H., Dawid, I. B. and Kawakami, K. (1998). Overexpression of the forebrain-specific homeobox gene six3 induces rostral forebrain enlargement in zebrafish. *Development* **125**, 2973-2982.

Kreitzer, A. C. and Malenka, R. C. (2008). Striatal plasticity and basal ganglia circuit function. *Neuron* **60**, 543-554.

Lagutin, O. V., Zhu, C. C., Kobayashi, D., Topczewski, J., Shimamura, K., Puelles, L., Russell, H. R., McKinnon, P. J., Solnica-Krezel, L. and Oliver, G. (2003). Six3 repression of Wnt signaling in the anterior neuroectoderm is essential for vertebrate forebrain development. *Genes Dev.* **17**, 368-379.

Lavado, A. and Oliver, G. (2011). Six3 is required for ependymal cell maturation. *Development* **138**, 5291-5300.

Li, X., Sun, C., Lin, C., Ma, T., Madhavan, M. C., Campbell, K. and Yang, Z. (2011). The transcription factor Sp8 is required for the production of parvalbumin-expressing interneurons in the olfactory bulb. *J. Neurosci.* **31**, 8450-8455.

Li, J., Wang, C., Zhang, Z., Wen, Y., An, L., Liang, Q., Xu, Z., Wei, S., Li, W., Guo, T. et al. (2017). Transcription factors Sp8 and Sp9 coordinately regulate olfactory bulb interneuron development. *Cereb. Cortex*, 1-17.

Liu, W., Lagutin, O. V., Mende, M., Streit, A. and Oliver, G. (2006). Six3 activation of Pax6 expression is essential for mammalian lens induction and specification. *EMBO J.* **25**, 5383-5395.

Liu, F., You, Y., Li, X., Ma, T., Nie, Y., Wei, B., Li, T., Lin, H. and Yang, Z. (2009). Brain injury does not alter the intrinsic differentiation potential of adult neuroblasts. *J. Neurosci.* **29**, 5075-5087.

Lobo, M. K., Karsten, S. L., Gray, M., Geschwind, D. H. and Yang, X. W. (2006). FACS-array profiling of striatal projection neuron subtypes in juvenile and adult mouse brains. *Nat. Neurosci.* **9**, 443-452.

Lobo, M. K., Yeh, C. and Yang, X. W. (2008). Pivotal role of early B-cell factor 1 in development of striatonigral medium spiny neurons in the matrix compartment. *J. Neurosci. Res.* **86**, 2134-2146.

Long, J. E., Garel, S., Alvarez-Dolado, M., Yoshikawa, K., Osumi, N., Alvarez-Buylla, A. and Rubenstein, J. L. R. (2007). Dlx-dependent and -independent regulation of olfactory bulb interneuron differentiation. *J. Neurosci.* **27**, 3230-3243.

Long, J. E., Swan, C., Liang, W. S., Cobos, I., Potter, G. B. and Rubenstein, J. L. R. (2009). Dlx1&2 and Mash1 transcription factors control striatal patterning and differentiation through parallel and overlapping pathways. *J. Comp. Neurol.* **512**, 556-572.

Loosli, F., Winkler, S. and Wittbrodt, J. (1999). Six3 overexpression initiates the formation of ectopic retina. *Genes Dev.* **13**, 649-654.

Lu, K.-M., Evans, S. M., Hirano, S. and Liu, F.-C. (2014). Dual role for Islet-1 in promoting striatonigral and repressing striatopallidal genetic programs to specify striatonigral cell identity. *Proc. Natl. Acad. Sci. USA* **111**, E168-E177.

Ma, T., Zhang, Q., Cai, Y., You, Y., Rubenstein, J. L. R. and Yang, Z. (2012). A subpopulation of dorsal lateral/caudal ganglionic eminence-derived neocortical interneurons expresses the transcription factor Sp8. *Cereb. Cortex* **22**, 2120-2130.

Ma, T., Wang, C., Wang, L., Zhou, X., Tian, M., Zhang, Q., Zhang, Y., Li, J., Liu, Z., Cai, Y. et al. (2013). Subcortical origins of human and monkey neocortical interneurons. *Nat. Neurosci.* **16**, 1588-1597.

Maia, T. V. and Frank, M. J. (2011). From reinforcement learning models to psychiatric and neurological disorders. *Nat. Neurosci.* **14**, 154-162.

Matsumoto, S., Yamazaki, C., Masumoto, K.-H., Nagano, M., Naito, M., Soga, T., Hiyama, H., Matsumoto, M., Takasaki, J., Kamohara, M. et al. (2006). Abnormal development of the olfactory bulb and reproductive system in mice lacking prokineticin receptor PKR2. *Proc. Natl. Acad. Sci. USA* **103**, 4140-4145.

McKenna, W. L., Betancourt, J., Larkin, K. A., Abrams, B., Guo, C., Rubenstein, J. L. R. and Chen, B. (2011). Tbr1 and Fezf2 regulate alternate corticofugal neuronal identities during neocortical development. *J. Neurosci.* **31**, 549-564.

McKinsey, G. L., Lindtner, S., Trzcinski, B., Visel, A., Pennacchio, L. A., Huylebroeck, D., Higashi, Y. and Rubenstein, J. L. R. (2013). Dlx1&2-dependent expression of Zfhx1b (Sip1, Zeb2) regulates the fate switch between cortical and striatal interneurons. *Neuron* **77**, 83-98.

Merchan-Sala, P., Nardini, D., Waclaw, R. R. and Campbell, K. (2017). Selective neuronal expression of the SoxE factor, Sox8, in direct pathway striatal projection neurons of the developing mouse brain. *J. Comp. Neurol.* **525**, 2805-2819.

Ng, K. L., Li, J. D., Cheng, M. Y., Leslie, F. M., Lee, A. G. and Zhou, Q. Y. (2005). Dependence of olfactory bulb neurogenesis on prokineticin 2 signaling. *Science* **308**, 1923-1927.

Oliver, G., Mailhos, A., Wehr, R., Copeland, N. G., Jenkins, N. A. and Gruss, P. (1995). Six3, a murine homologue of the sine oculis gene, demarcates the most anterior border of the developing neural plate and is expressed during eye development. *Development* **121**, 4045-4055.

Ragancokova, D., Rocca, E., Oonk, A. M. M., Schulz, H., Rohde, E., Bednarsch, J., Feenstra, I., Pennings, R. J. E., Wende, H. and Garratt, A. N. (2014). TSHZ1-dependent gene regulation is essential for olfactory bulb development and olfaction. *J. Clin. Invest.* **124**, 1214-1227.

Rubenstein, J. L. R. and Campbell, K. (2013). Neurogenesis in the Basal Ganglia. In *Patterning and Cell Type Specification in the Developing CNS and PNS*, Vol. 1, pp. 455-473 (ed. J. L. R. Rubenstein and P. Rakic). Amsterdam, The Netherlands: Elsevier.

Sandberg, M., Flandin, P., Silberberg, S., Su-Feher, L., Price, J. D., Hu, J. S., Kim, C., Visel, A., Nord, A. S. and Rubenstein, J. L. R. (2016). Transcriptional networks controlled by NKX2-1 in the development of forebrain GABAergic neurons. *Neuron* **91**, 1260-1275.

Sheth, A. N. and Bhide, P. G. (1997). Concurrent cellular output from two proliferative populations in the early embryonic mouse corpus striatum. *J. Comp. Neurol.* **383**, 220-230.

Shirasaki, D. I., Greiner, E. R., Al-Ramahi, I., Gray, M., Boontheung, P., Geschwind, D. H., Botas, J., Coppola, G., Horvath, S., Loo, J. A. et al. (2012). Network organization of the huntingtin proteomic interactome in mammalian brain. *Neuron* **75**, 41-57.

Silberberg, S. N., Taher, L., Lindtner, S., Sandberg, M., Nord, A. S., Vogt, D., McKinsey, G. L., Hoch, R., Pattabiraman, K., Zhang, D. et al. (2016). Subpallial enhancer transgenic lines, a data and tool resource to study transcriptional regulation of GABAergic cell fate. *Neuron* **92**, 59-74.

Smart, I. H. (1976). A pilot study of cell production by the ganglionic eminences of the developing mouse brain. *J. Anat.* **121**, 71-84.

Stenman, J., Toresson, H. and Campbell, K. (2003). Identification of two distinct progenitor populations in the lateral ganglionic eminence: implications for striatal and olfactory bulb neurogenesis. *J. Neurosci.* **23**, 167-174.

Toresson, H. and Campbell, K. (2001). A role for Gsh1 in the developing striatum and olfactory bulb of Gsh2 mutant mice. *Development* **128**, 4769-4780.

Trapnell, C., Roberts, A., Goff, L., Pertea, G., Kim, D., Kelley, D. R., Pimentel, H., Salzberg, S. L., Rinn, J. L. and Pachter, L. (2012). Differential gene and transcript expression analysis of RNA-seq experiments with TopHat and Cufflinks. *Nat. Protoc.* **7**, 562-578.

Tronche, F., Kellendonk, C., Kretz, O., Gass, P., Anlag, K., Orban, P. C., Bock, R., Klein, R. and Schütz, G. (1999). Disruption of the glucocorticoid receptor gene in the nervous system results in reduced anxiety. *Nat. Genet.* **23**, 99-103.

Waclaw, R. R., Allen, Z. J., II, Bell, S. M., Erdélyi, F., Szabó, G., Potter, S. S. and Campbell, K. (2006). The zinc finger transcription factor Sp8 regulates the generation and diversity of olfactory bulb interneurons. *Neuron* **49**, 503-516.

Xu, Q., Guo, L., Moore, H., Waclaw, R. R., Campbell, K. and Anderson, S. A. (2010). Sonic hedgehog signaling confers ventral telencephalic progenitors with distinct cortical interneuron fates. *Neuron* **65**, 328-340.

Yun, K., Fischman, S., Johnson, J., Hrabe de Angelis, M., Weinmaster, G. and Rubenstein, J. L. (2002). Modulation of the notch signaling by Mash1 and Dlx1/2 regulates sequential specification and differentiation of progenitor cell types in the subcortical telencephalon. *Development* **129**, 5029-5040.

Zhang, Q., Zhang, Y., Wang, C., Xu, Z., Liang, Q., An, L., Li, J., Liu, Z., You, Y., He, M. et al. (2016). The zinc finger transcription factor Sp9 is required for the development of striatopallidal projection neurons. *Cell Rep.* **16**, 1431-1444.

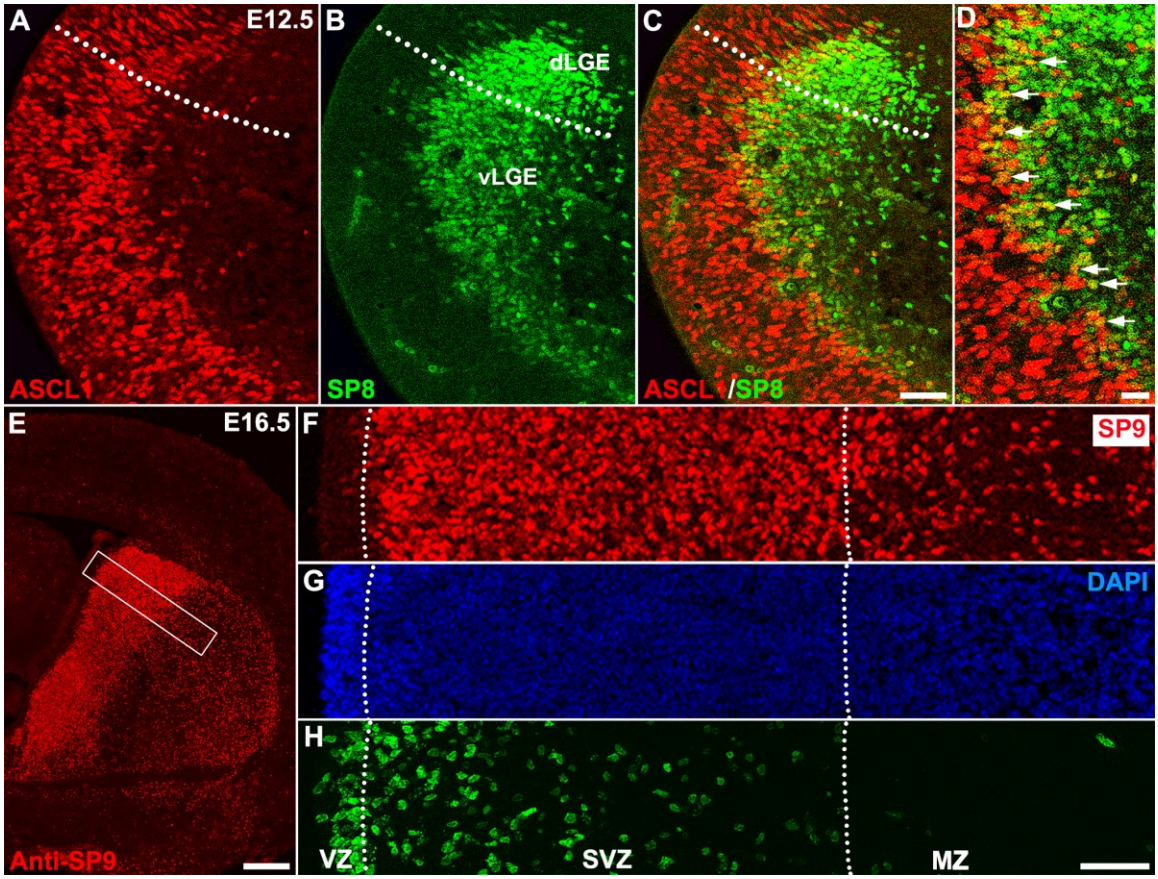

Fig. S1. A few SP8^{+} cells in the LGE SVZ express ASCL1 at E12.5. (A-C) SP8/ASCL1 double immunostained coronal LGE sections at E12.5. **(D)** Higher magnification image showing that a few SP8^{+}/ASCL1^{+} cells (arrows) are present in the LGE SVZ. **(E, F)** Strong SP9 expression in the LGE SVZ and MZ (mantle zone, striatum) at E16.5. (**G, H**). The anatomical borders of the VZ/SVZ/MZ are based DAPI and BrdU staining (BrdU 30 min pulse labeling). Scale bars: 50 μm in **C** for **A-C**; 20 μm in **D**; 200 μm in **E**; 50 μm in **H** for **F-H**.

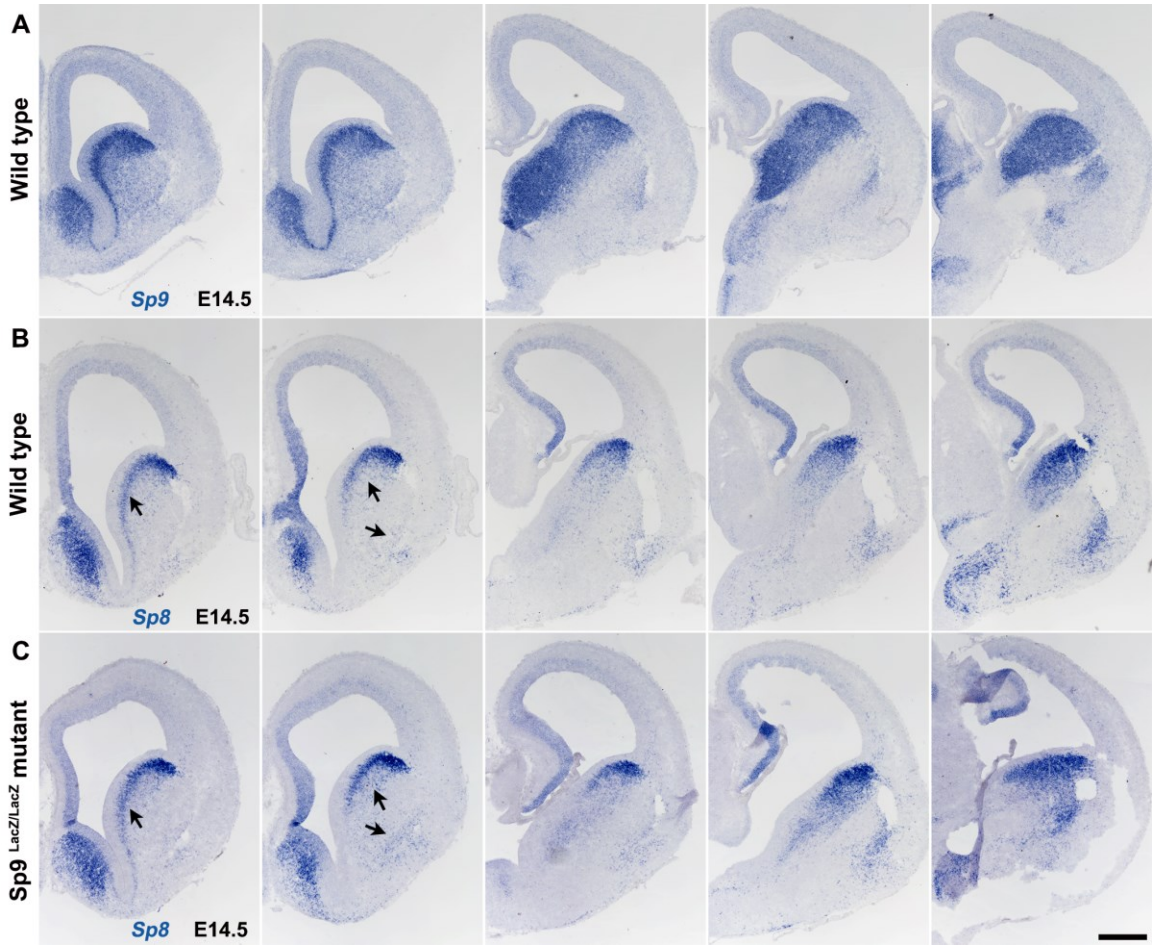

Fig. S2. *Sp8* expression is upregulated in the LGE SVZ of *Sp9* mutant mice at E14.5. (A-C) *In situ* RNA hybridization analysis of *Sp8* and *Sp9* expression in whole hemisphere sections at E14.5 (rostral-most on the left). Note upregulation of *Sp8* expression in the *Sp9-KO* LGE (arrows), compared with wild type controls. Scale bar: 400 µm.

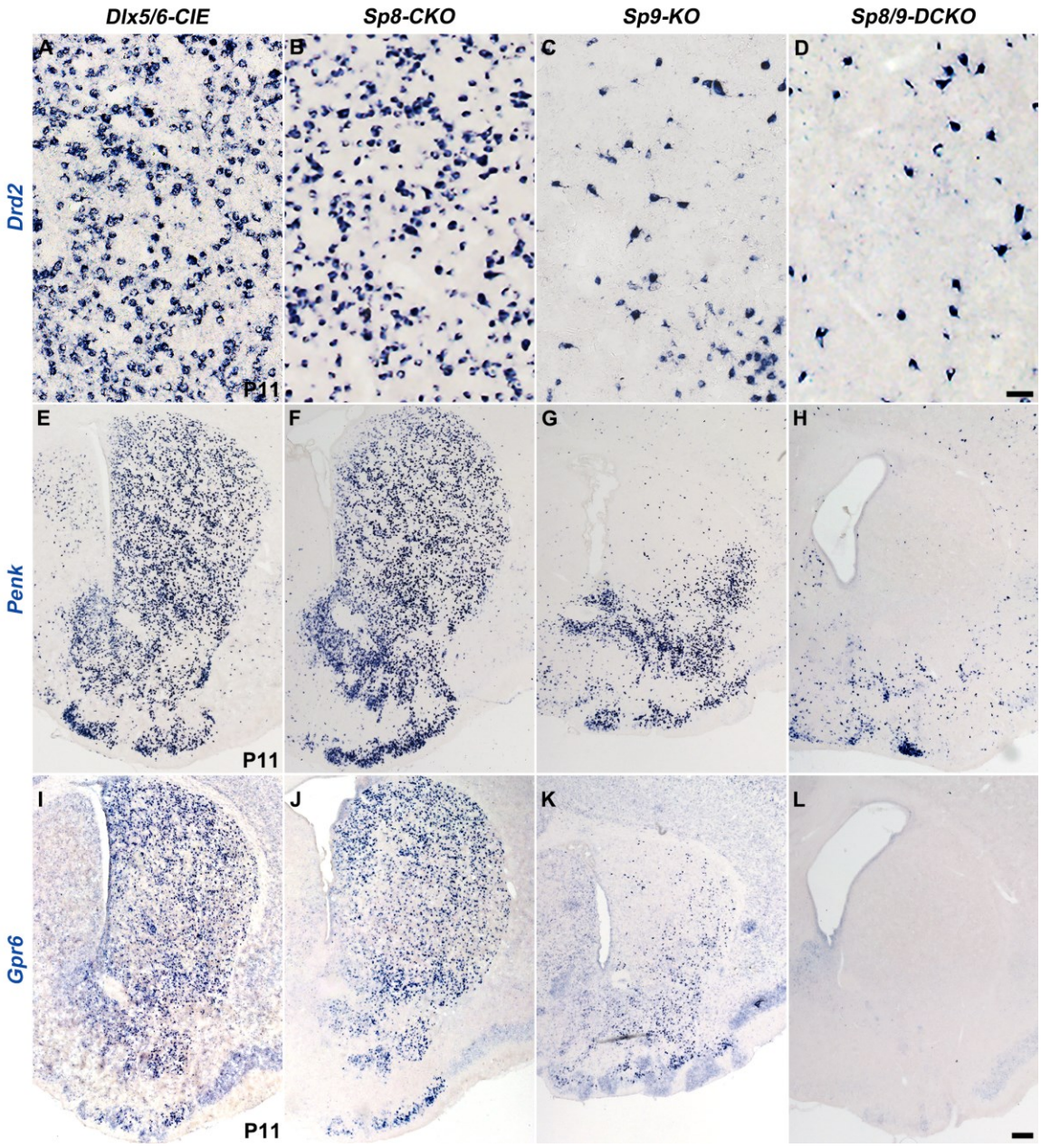

Fig. S3. D2 MSNs are lost in the striatum of *Sp8/9-DCKO* mice. (A-D) Higher magnification images of *Drd2*$^{+}$ cells in the striatum of control and mutant mice at P11. Those remaining *Drd2*$^{+}$ cells in the striatum of *Sp8/9-DCKO* mice are ChAT^{+} interneurons; note those *Drd2*$^{+}$ cells with a much larger soma size **(C, D**). **(E-L**) In situ RNA hybridization of *Penk* and *Gpr6* showing loss of D2 MSNs in *Sp8/9-DCKO* mice at P11. Scale bars: 50 µm in **D** for **A-D**; 200 µm in **L** for **E-L**.

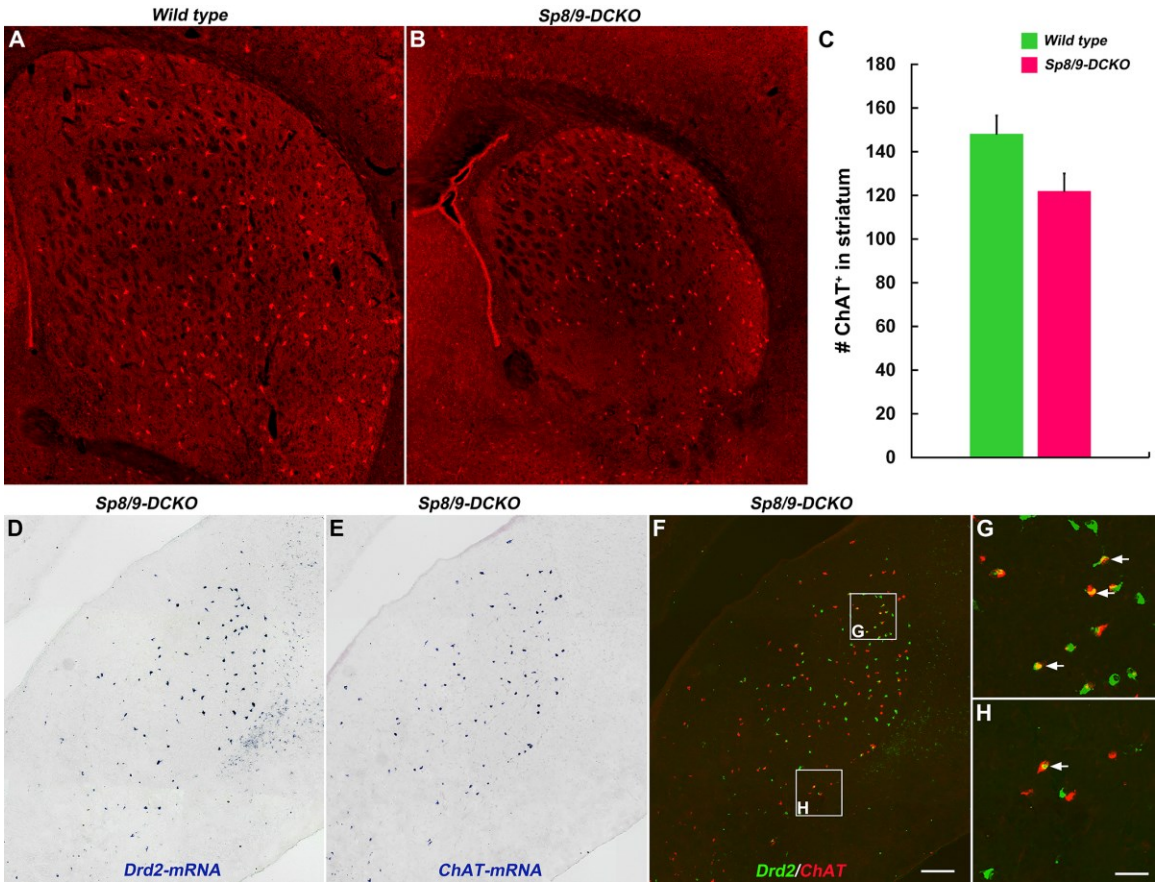

Fig. S4. Drd2$^+$ cells in the *Sp8/9-DCKO* striatum are ChAT$^+$ interneurons. (A-C) Compared with wild type controls, ChAT$^+$ striatal interneurons are less affected in the *Sp8/9-DCKO* mice. (**D-F**) Those remaining Drd2$^+$ cells in the striatum of *Sp8/9-DCKO* mice are ChAT$^+$ interneurons. *Drd2* and *ChAT* double in situ image (**F**) was composed from immediate adjacent 20 μm sections (**D and E**) using Adobe Photoshop. (**G, H**) Higher magnification images of boxed areas in **(F)** showing *Drd2*$^+$/*ChAT*$^+$ cells (arrows) Scale bars: 200 μm in **F** for **A-F**; 50 μm in **H** for **G, H**.

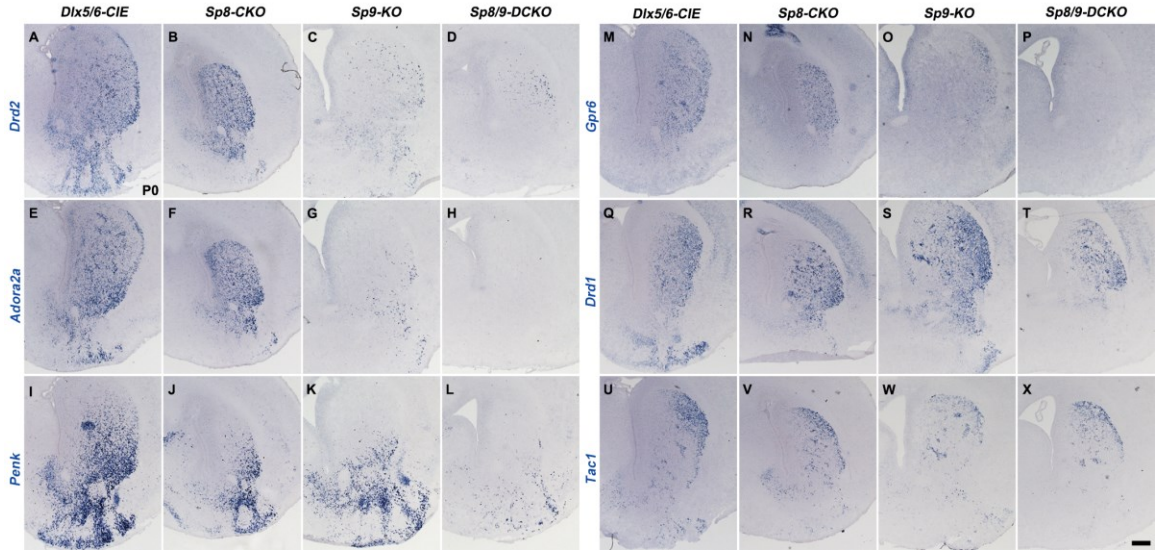

Fig. S5. D1 and D2 MSNs in the striatum of *Sp8-CKO, Sp9-KO* and *Sp8/9-DCKO* mice at P0. (A-X) *In situ* RNA hybridization of *Drd2*, *Adora2a*, *Penk, Gpr6, Drd1* and *Tac1* in the striatum of control and mutants at P0. D2 MSNs are lost in the striatum of *Sp8/9-DCKO* mice (**D, H, L, P**). D1 MSN development is largely unaffected in these mutant mice (**Q-X**). Scale bar: 200 μm.

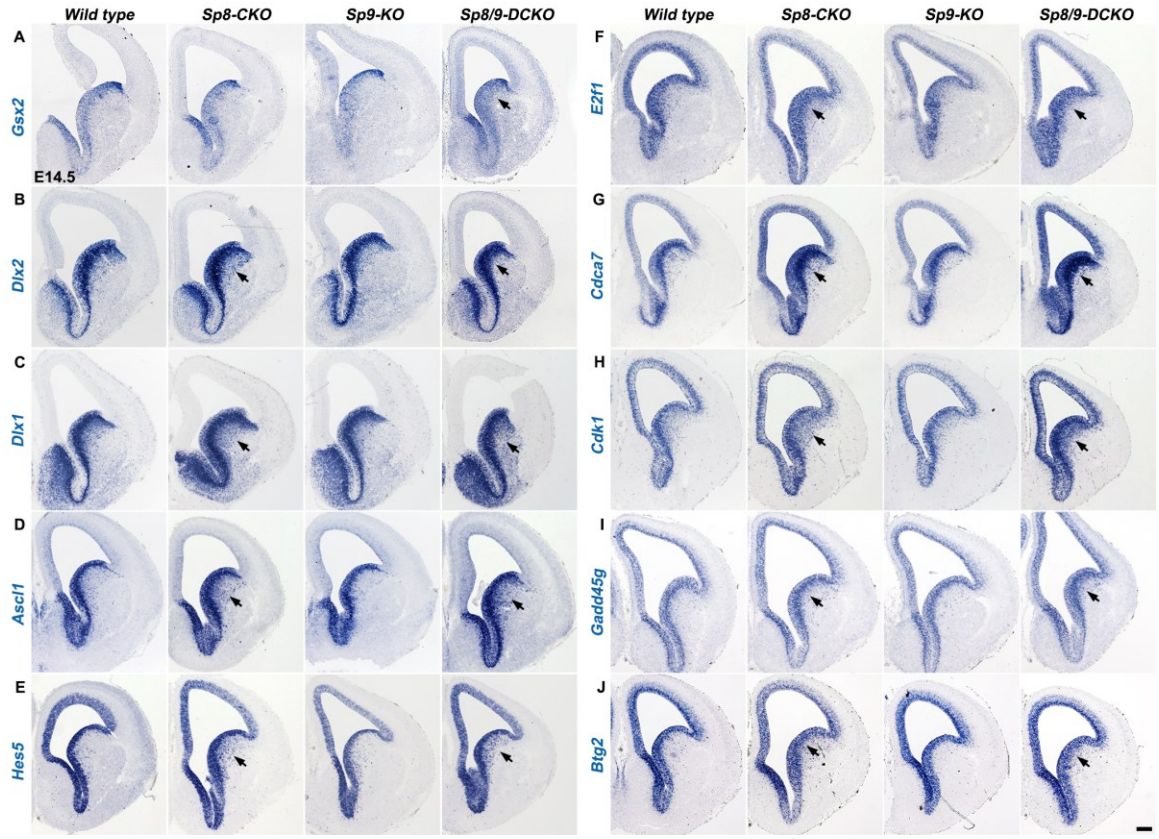

Fig. S6. Increased expression of *Gsx2*, *Dlx2, Dlx1, and Ascl1,* and its target genes, in the LGE of *Sp8-CKO* and *Sp8/9-DCKO* mice. (A-J) Expression of *Gsx2*, *Dlx2*, *Dlx1*, *Ascl1* and selected *Ascl1* target genes (*Hes5*, *E2f1*, *Cdca7*, *Cdk1*, *Gadd45g* and *Btg2*) were increased in the LGE VZ/SVZ of *Sp8-CKO* and *Sp8/9-DCKO* mice (arrows), but not in the LGE of *Sp9-KO* mice at E14.5. Scale bar: 200 μm.

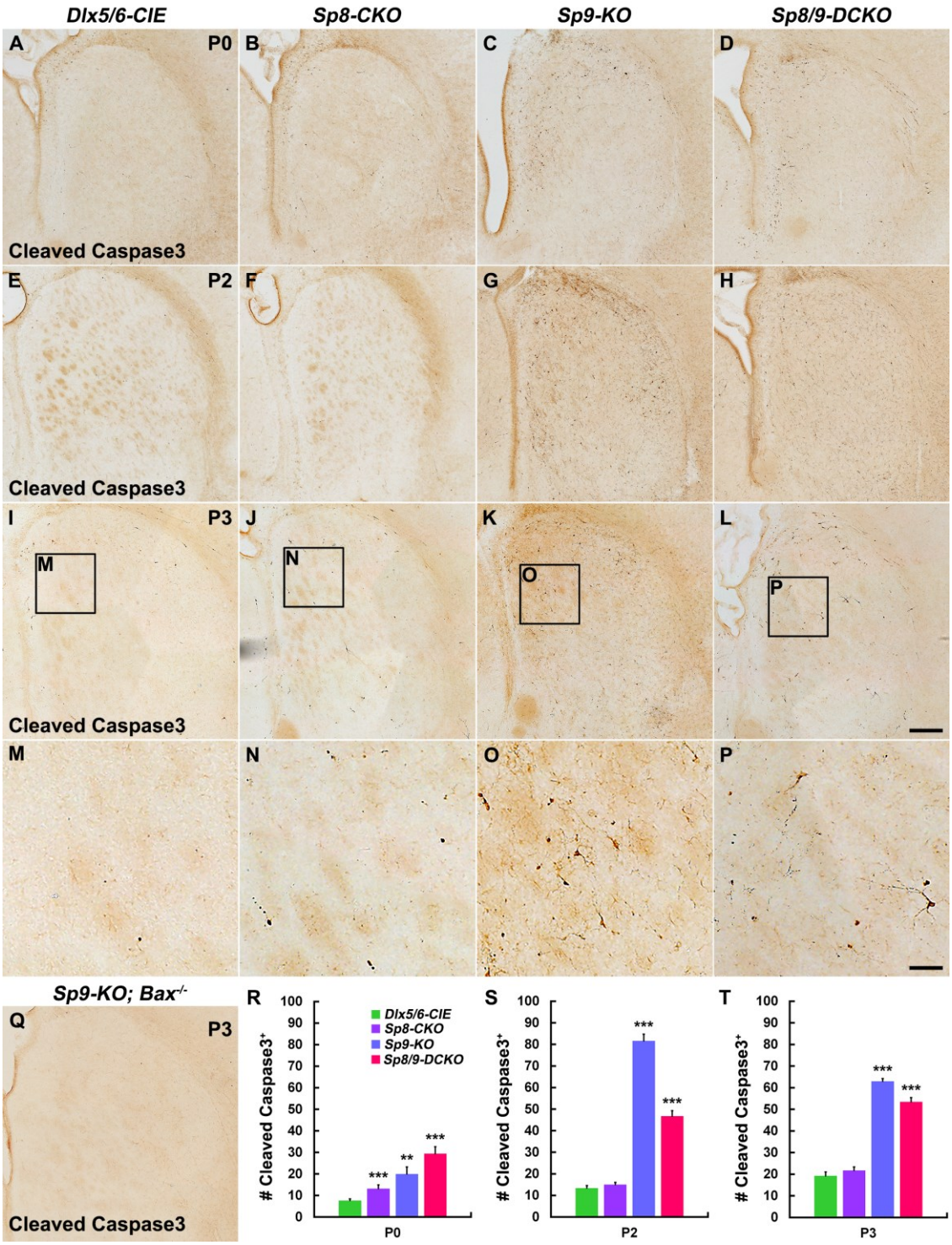

Fig. S7. Apoptosis occurs in the striatum of *Sp8-CKO, Sp9-KO* and *Sp8/9-DCKO* mice. (A-P) There were more Cleaved Caspase-3^{+} cells in the mutant striatum compared with controls (Dlx5/6-CIE) at P0, P2 and P3. (**Q**) Caspapse-3^{+} cells were not observed in the striatum of *Sp9-KO; Bax*$^{-/-}$ mice. Note more Caspapse-3^{+} cells in the striatum of *Sp9-KOs* than *Sp8/9-DCKOs* at P2 and P3. (one-way ANOVA followed by Tukey-Kramer post hoc test, ** $p < 0.01$, *** $p < 0.001$, n = 3, mean ± SEM). Scale bars: 200 μm in **L** for **A-L, Q**; 50 μm in **P** for **M-P**.

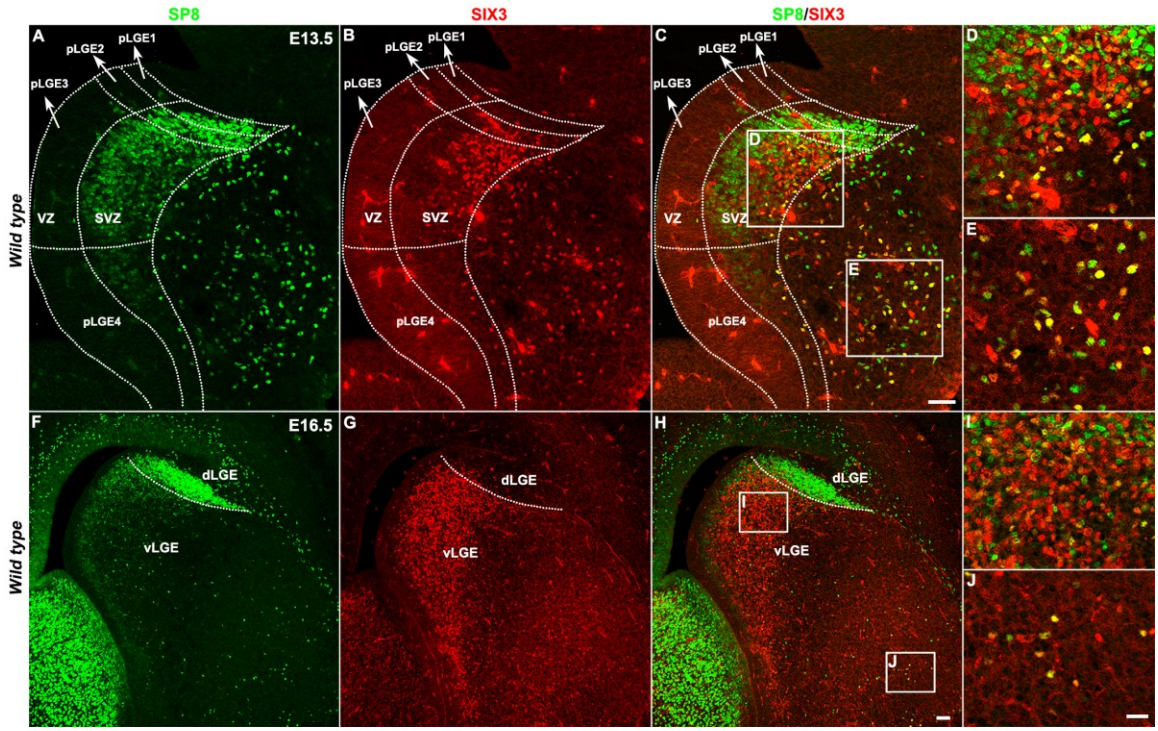

Fig. S8. SIX3 is mainly expressed in the dorsal part of the vLGE. (A-C) SIX3/SP8 double immunostaining shows that SIX3 is expressed in the dorsal part of the vLGE, putative pLGE3 SVZ, but not in the dLGE (pLGE1&2 SVZ) at E13.5 wild type mice. Note that SP8 is strongly expressed in the dLGE SVZ (pLGE1&2) and weakly expressed in the vLGE SVZ (pLGE3). **(F-H**) SIX3/SP8 double immunostaining shows that SIX3 is expressed in the vLGE, but not in the dLGE at E16.5. Again, SP8 is strongly expressed in the dLGE SVZ and weakly expressed in the vLGE SVZ. Note higher magnification images of $SP8^{+}/SIX3^{+}$ cells in the LGE SVZ and MZ (**D, E, I, J**). Scale bars: 50 μm in **C** for **A-C**; 50 μm in **H** for **F-H**; 50 μm in **J** for **D, E, I, J.**

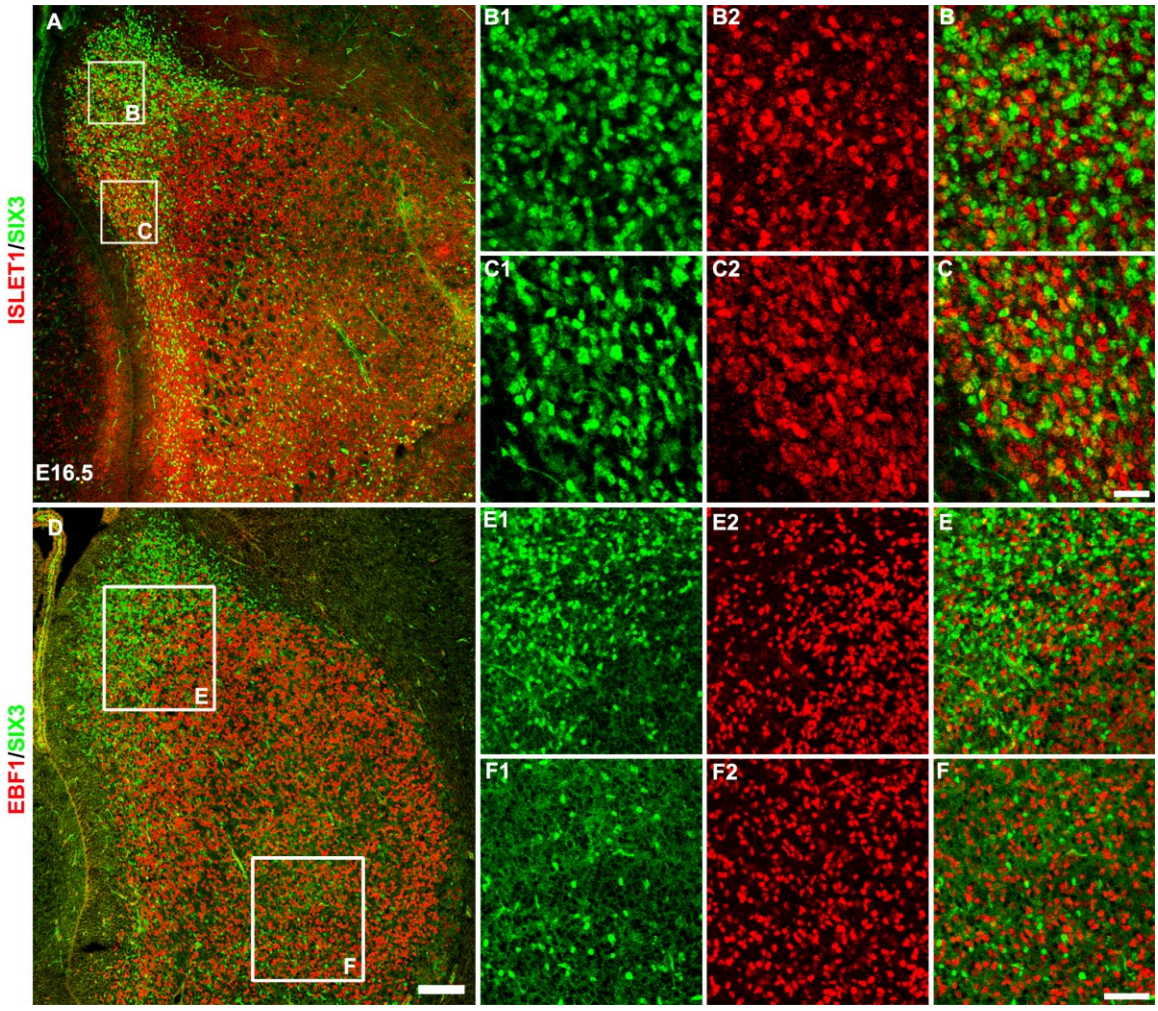

Fig. S9. SIX3 is not expressed in ISL1^{+} or EBF1^{+} cells in the LGE. (A, D) Immunostaining of SIX3, EBF1 and ISL1 in the LGE sections at E16.5. **(B, C, E, F)** Higher magnification images of boxed areas in (**A, D**) showing that very few SIX3^{+} cells express EBF1 or ISL1. Scale bars: 100 μm in **D** for **A, D**; 20 μm in **C** for **B1-C;** 50 μm in **F** for **E1-F**.

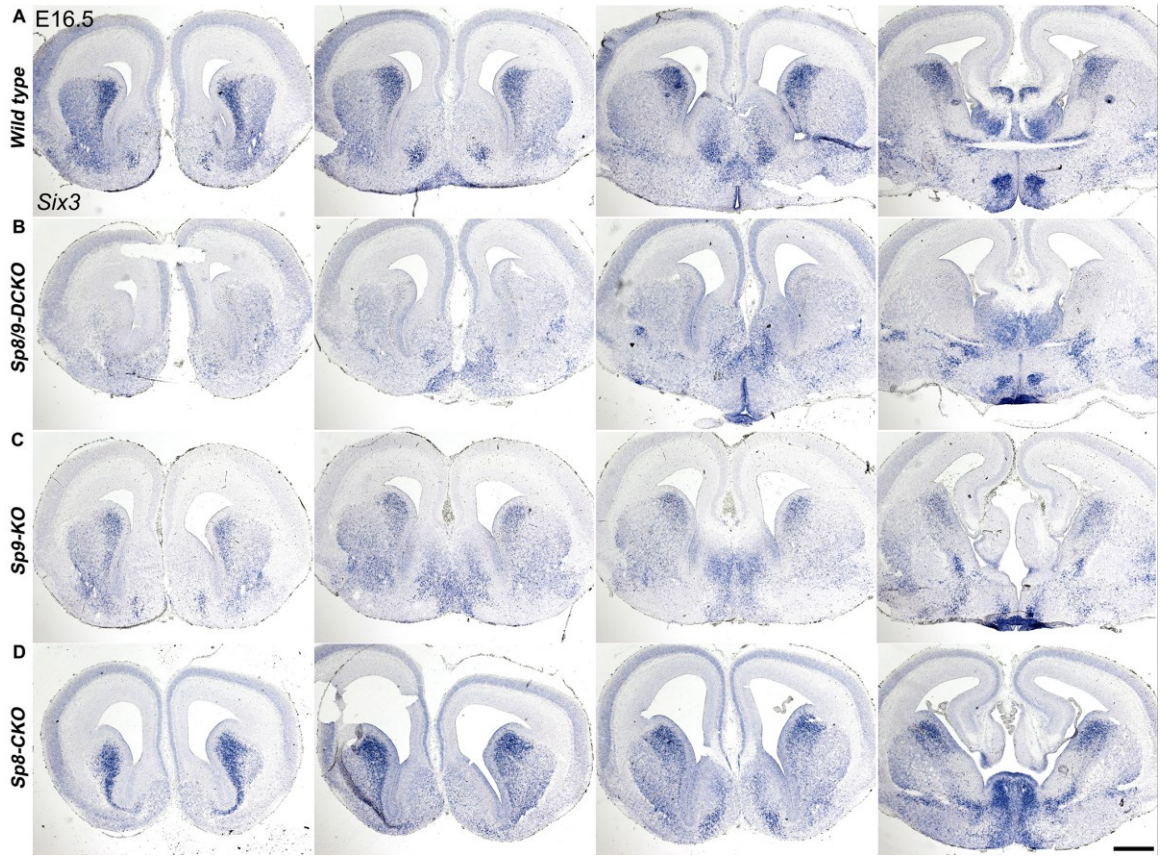

Fig. S10. *Six3* expression is lost in the LGE SVZ of *Sp8/9-DCKO* mice. (A-D) In situ RNA hybridization analysis of *Six3* expression in *wild type*, *Sp8-CKO*, *Sp9-KO* and *Sp8/9-DCKO* mice at E16.5. Four serial coronal sections (rostral-most on the left) are shown. Scale bar: 500 µm.

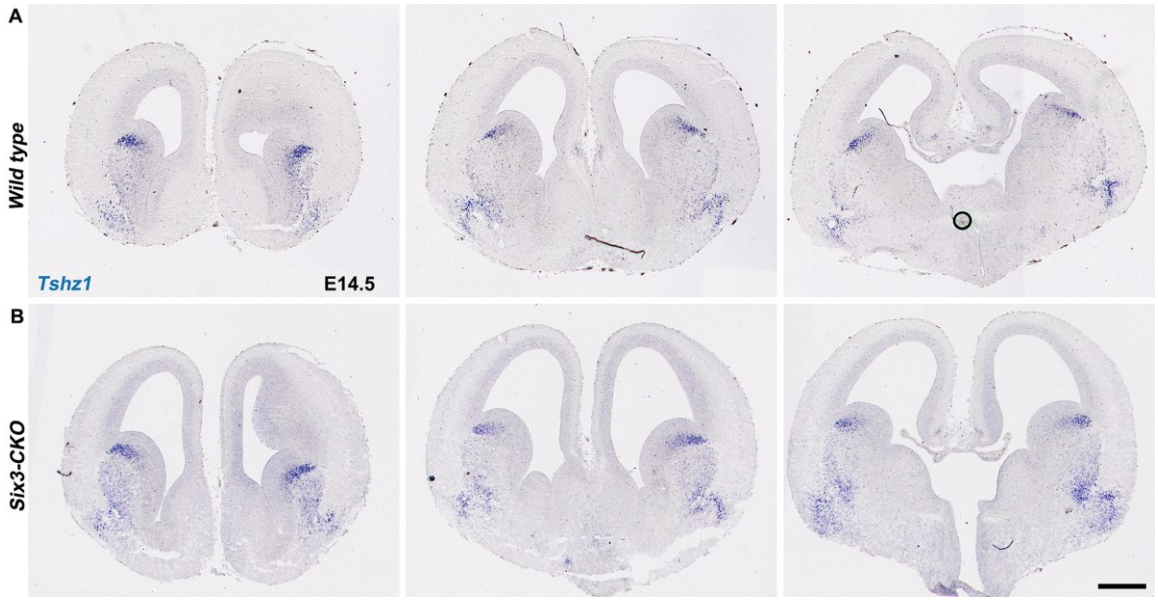

Fig. S11. *Tshz1* is expressed in the LGE SVZ of *Six3-CKO* mice. (A, B) *In situ* RNA hybridization analysis of *Tshz1* expression in the LGE of wild type controls and *Six3-CKO* mice at E14.5. Three serial coronal sections (rostral-most on the left) are shown. Note slight increased *Tshz1* expression in the dLGE SVZ of *Six3-CKO* mice (**B**), compared with wild type controls (**A**). Scale bar: 500 μm.

Table S1. Effect of *Sp8/9* Deletion on Expression Levels of Genes Related to LGE Development at E16.5

Gene Name	Sp8/9-DCKO FPKM	Control FPKM	Fold Change Mutant/Control	P_value	FDR	UP/DOWN Regulation
Sp8	0.67626	7.71221	0.087697	0.020513	1	DOWN
Sp9	1.42512	137.825	0.010340	2.61E-39	1.60E-35	DOWN
			D2-MSN			
Adora2a	2.25904	35.1088	0.064344	1.56E-08	1.60E-05	DOWN
Drd2	1.53835	26.6066	0.057818	7.30E-07	0.000449	DOWN
Gpr6	1.00E-05	5.10827	1.96E-06	0.068136	1	DOWN
Penk	0.565026	8.67965	0.065098	0.011104	1	DOWN
Ptprm	2.21765	15.7722	0.140605	0.002395	0.490505	DOWN
Six3	12.7351	64.2185	0.198309	8.57E-10	0.000001	DOWN
Grik3	7.34664	41.8135	0.175700	5.79E-07	0.000395	DOWN
Gucy1a3	34.1785	112.847	0.302875	3.08E-11	5.17E-08	DOWN
Gucy1b3	31.0887	67.2435	0.462330	0.000276	0.080671	DOWN
Mpped2	55.1883	133.887	0.412201	6.14E-09	7.08E-06	DOWN
Syt6	37.9725	79.5554	0.477309	9.36E-05	0.035205	DOWN
Tle4	12.7052	32.8424	0.386854	0.002894	0.573583	DOWN
Zfhx3	10.711	23.9544	0.447141	0.027704	1	DOWN
Elmo1	14.2729	28.5504	0.499919	0.034462	1	DOWN
			D1-MSN			
Chrm4	6.67332	6.77617	0.984822	1	1	DOWN
Drd1	8.03876	6.82957	1.177052	0.803722	1	UP
Ebf1	82.7113	102.822	0.804412	0.123563	1	DOWN
Gnb4	20.6071	23.4174	0.879991	0.656580	1	DOWN
Isl1	85.8251	88.1986	0.973089	0.762648	1	DOWN
Nrxn1	25.2266	23.9241	1.054443	0.887908	1	UP
Pdyn	2.53387	2.80708	0.902671	1	1	DOWN
Sfxn1	24.3366	20.7232	1.174365	0.659222	1	UP
Sox8	75.6229	84.499	0.894956	0.431328	1	Down
Tac1	99.9393	73.3854	1.361842	0.068641	1	UP
			Progenitor			
Ascl1	91.6101	56.6476	1.617193	0.006666	1	UP
Dbi	691.661	445.835	1.551383	2.13E-12	4.37E-09	UP
Dlx1	168.624	138.782	1.215028	0.123879	1	UP
Dlx2	226.047	158.155	1.429275	0.001094	0.258622	UP
Fabp7	1306.74	812.26	1.608771	2.63E-25	9.68E-22	UP
Gsx1	9.52869	2.01106	4.738143	0.092422	1	UP
Gsx2	20.076	10.3295	1.94356	0.110555	1	UP
Lhx2	55.2738	25.571	2.161581	0.001257	0.289621	UP
Nes	47.4698	37.4409	1.267859	0.333196	1	UP
Nfix	55.3995	35.1904	1.574279	0.047673	1	UP
Vim	276.424	216.593	1.276237	0.013231	1	UP
			Neuron			
Bcl11a	121.535	181.456	0.669777	0.000362	0.096688	DOWN
Bcl11b	164.558	233.749	0.703994	0.000304	0.083653	DOWN
Dcx	133.411	194.039	0.687547	0.000495	0.128592	DOWN
Foxg1	255.161	302.222	0.844283	0.030880	1	DOWN
Foxp1	99.3202	159.366	0.623221	0.000115	0.040722	DOWN

Gad1	39.8202	81.2468	0.490114	0.000123	0.042895	DOWN
Id4	68.8989	132.036	0.521819	4.00E-06	0.001995	DOWN
Meis2	156.4	226.855	0.689427	0.000189	0.058185	DOWN
Nnat	1372.04	1746.46	0.785612	7.78E-13	1.79E-09	DOWN
Nrep	545.997	666.685	0.818973	0.000185	0.057821	DOWN
Nsg2	492.615	602.407	0.817744	0.000357	0.096846	DOWN
Rxrg	74.023	102.671	0.720973	0.029565	1	DOWN
Sox11	402.371	454.46	0.885383	0.047516	1	DOWN
Sox4	445.308	501.185	0.88851	0.040580	1	DOWN
Tuba1a	632.331	731.696	0.864199	0.002880	0.577027	DOWN
Tubb2b	833.706	973.94	0.856014	0.000286	0.081153	DOWN
Tubb3	929.682	1230.69	0.755415	6.84E-12	1.26E-08	DOWN
			Ascl1-Related			
Ascl1	91.6101	56.6476	1.617193	0.006666	1	UP
Birc5	42.9451	32.4368	1.323962	0.303075	1	UP
Btg2	26.3267	16.5884	1.587055	0.174791	1	UP
Ccnd2	354.846	274.316	1.293567	0.003154	0.61845	UP
Ccng2	98.425	106.394	0.925099	0.530758	1	DOWN
Cdc25b	20.8923	15.5989	1.339344	0.511890	1	UP
Cdca7	172.32	89.1914	1.932025	6.64E-07	0.000422	UP
Cdk1	22.6534	16.1246	1.404897	0.430197	1	UP
Cdk2	18.0002	12.8934	1.396079	0.377588	1	UP
Cdkn1a	10.6733	3.94016	2.708849	0.118649	1	UP
Cdkn1c	11.1874	16.2148	0.68995	0.358098	1	DOWN
Cdkn2a	0.0281095	0.05805	0.484246	1	1	DOWN
Cdkn2b	0.681231	0.52006	1.309906	1	1	UP
Cdkn2c	15.4188	10.5131	1.466627	0.442475	1	UP
Cdkn2d	40.2965	34.9139	1.154168	0.567540	1	UP
Cdkn3	4.62482	3.2143	1.438826	1	1	UP
Cyr61	13.2597	10.3431	1.281985	0.690281	1	UP
Dll1	19.2025	15.9974	1.200351	0.618136	1	UP
Dll3	24.5785	13.9649	1.76002	0.108578	1	UP
E2f1	16.5704	12.285	1.348832	0.585037	1	UP
Ebf3	2.92111	0.42517	6.87042	0.625049	1	UP
Ep400	23.5151	25.6166	0.917963	0.778355	1	DOWN
Fbxw7	19.8917	17.8833	1.112306	0.871574	1	UP
Foxm1	29.2052	22.805	1.280649	0.410917	1	UP
Gadd45g	110.398	59.2614	1.862899	0.000163	0.053599	UP
Gpc1	90.7377	117.083	0.774986	0.052524	1	DOWN
Hes1	8.34294	6.53633	1.276395	0.803722	1	UP
Hes5	55.0925	31.3784	1.755746	0.014021	1	UP
Hes6	85.2984	64.6601	1.319181	0.121794	1	UP
Hipk2	21.1973	17.7752	1.192521	0.636273	1	UP
Id1	11.269	7.39994	1.52285	0.503727	1	UP
Id3	8.99242	7.85163	1.145293	1	1	UP
Notch1	37.5689	28.9562	1.297439	0.329494	1	UP
Notch2	16.7376	12.2635	1.364831	0.585037	1	UP
Notch3	15.6126	11.0084	1.418244	0.571944	1	UP
Skp2	21.4739	16.633	1.291042	0.522931	1	UP
Tead1	20.5639	16.1002	1.277245	0.627534	1	UP
Tead2	60.2986	44.3749	1.358845	0.146174	1	UP
Wwtr1	12.7674	8.95877	1.425129	0.523769	1	UP